63 3-3

OCF
NOrd 15764
PAA-4
c.2

INVESTIGATION OF GLASS-METAL COMPOSITE MATERIALS

P. A. Lockwood

Contract NOrd 15764

Fourth Annual Progress Report

Covering Period March 15, 1958 to June 15, 1959

(Also includes Thirteenth Quarterly Progress
Report)

ALL DISTRIBUTION OF THIS REPORT IS CONTROLLED.
QUALIFYING ASTIA USERS SHOULD REQUEST THROUGH
THE CHIEF, BUREAU OF NAVAL WEAPONS, WASHINGTON 25,
D. C.

Qualified requesters may.
obtain copies of this
report from ASTIA.

Owens-Corning FIBERGLAS Corporation
Basic and Applied Research Center
Newark, Ohio

ASTIA

APR 30 1963

TISI'

TABLE OF CONTENTS

LIST OF TABLES

LIST OF FIGURES

INVESTIGATION OF GLASS-METAL COMPOSITE MATERIALS

INTRODUCTION

This report covers research effort expended on Naval Ordnance Contract NOrd 15764 in the period March 15, 1958, to June 15, 1959. It comprises work reported in the Tenth, Eleventh, and Twelfth Quarterly Progress Reports and work performed in the period December 15, 1958, to June 15, 1959, inclusive of the thirteenth quarter for which a separate report will not be submitted. On January 21, 1959, the research facilities of the Owens-Corning Fiberglas Corporation at Newark, Ohio, were disrupted by a flood. Approximately three months were required to return the Laboratory to normal operating condition and to replace the considerable number of test specimens that were lost. By permission of Mr. George B. Butters, Contracting Officer, the reporting period for the Fourth Annual Progress Report was extended to June 15, 1959.

The major effort was directed to improving the characteristics of glass-metal composites by determining the variables affecting their behavior. One investigation was concerned with the factors controlling the strength of single filaments in the operation of forming and coating them with molten metals. In another investigation the physical properties of composite materials were examined in relation to the theories which have been evolved to explain or predict their behavior.

The work represents the combined effort of Messrs. J. I. Aber, R. E. Evans, P. A. Lockwood, E. E. Mattern, N. L. Leedy and Dr. H. B.

Whitehurst and Dr. J. W. Michener. Consulting work was done by Dr. Edward
Saibel of Rensselaer Polytechnic Institute and Dr. T. S. Shevlin of The
Ohio State University.

Physical property measurements of the glass-reinforced metal test
bars were performed at The Ohio State Experimental Station under the
direction of Dr. T. S. Shevlin and at the Owens-Corning Fiberglas Testing
Laboratories.

Invaluable assistance in the preparation of the text of this report
was given by Mr. J. A. Grant of the Research Laboratories administrative
staff of Owens-Corning Fiberglas.

SUMMARY

Work at the start of the fourth year of research on glass-metal composites was mainly directed to creating composites of acceptable strength-to-weight ratio suitable for service in the 1500 - 2000°F range.

Direct high temperature analogues of glass-aluminum composites could not be made by the techniques successful for glass-aluminum. Neither "E" glass nor fused silica fibers could be coated in the fiber-forming operation or vacuum injection cast with metals melting above aluminum. The alloys used, mainly those of copper, oxidized deeply and too rapidly and the fibers were excessively embrittled.

An adaptation of powder metallurgy techniques comprising mixing fibers with powdered metals, hot pressing into green compacts and sintering was explored with partial success. Samples of nickel, copper, stainless steel, chromium, and brass with "E" glass or fused silica fibers, both bare and aluminum coated, were carried through the green compact stage. Sintering was not satisfactorily accomplished due to equipment limitations. To overcome the difficulty, major expenditures for capital equipment were required and for that reason work on high temperature composites was temporarily discontinued.

A study was initiated to discover the underlying mechanisms responsible for the physical properties exhibited by glass-aluminum composites. Work was divided into two sections. In one, the factors controlling the strength of metal-coated fibers were investigated. In the other, the

properties of composites were examined to determine the interactions of glass and metal in producing the final composite properties.

To facilitate tensile testing of single fibers a multihead tester was developed capable of pulling eight fibers simultaneously and providing a trace record of stress versus time for each. The device provided the requisite sensitivity and greatly accelerated testing work.

Quality of metal coatings was found not to be a factor affecting fiber strengths. It had been assumed that thickness, smoothness and completeness of coatings correlated with higher fiber tensile strengths. In one series of experiments using three glasses varying from excellent to poor in coatability with two aluminum alloys, the coated fiber tensile strength was a constant percentage of the virgin fiber strength of each glass independent of coating quality. For 1100 aluminum the coated fiber tensile strength was 20 - 24 per cent of virgin fiber strength and for a 94 per cent aluminum - 5 per cent zinc - 1 per cent cadmium alloy, 17 - 23 per cent. In another series of experiments five parameters in the operation of fiber forming and metal coating believed to control coating quality and strength were studied. It was found that the parameters studied were not the only controlling ones; some other variable influenced coating thickness and tensile strength to a greater extent. Strengths were not reproducible in reruns. A set of parameters was established after much labor which would give reproducible and relatively even coatings of metal on the fibers. This was accomplished with a combination of relatively high pulling speed and careful metering of

metal flow. Tensile strength of fibers so produced was relatively low,
averaging 107,000 ± 8,000 psi.

The strength of aluminum-coated glass fiber was found to be affected
by humidity the same as bare glass fiber. Strength was 20 per cent greater
in 5 per cent relative humidity versus 60 per cent relative humidity
atmosphere. Lead-coated fibers were not so affected.

Experiments were performed on the thermal expansion of metal-coated
fibers and glass-metal composites. Efforts were made to correlate the
results with the treatise by R. B. Wiley on "Thermal Expansion of Glass-
Metal Composites."[1] The experiments were not decisive and correlation
was therefore not possible. More work under finer control is needed in
this area.

The properties of glass reinforced aluminum composites were compared
with those of sintered aluminum powder (SAP) with the object of deter-
mining if the mechanisms by which the matrix metal of each are reinforced
are the same or different. The results indicated that glass-aluminum
composites had properties which were similar or superior to those of the
SAP materials but that the mechanisms were not the same. The tensile
strength of glass-aluminum composites is achieved at interparticle
spacings considerably larger than the theoretical minimum required by
SAP materials theory. This became apparent only at elevated temperatures.
The difference was enhanced with increasing glass content and was taken
to indicate that the factor determining the minimum tensile strength of

[1]Eleventh Quarterly Progress Report. Contract NOrd 15764, June 15,
1958, to September 15, 1958.

glass-aluminum composites is dependent on the presence of the glass in filamentous form. Since the comparison is made on the basis of the observation that the tensile strength of SAP materials is dependent on inter-particle spacing of the oxide particles, no conclusion can be drawn regarding the mechanism operating in the fiber reinforced materials. Two other basic differences in behavior between the two materials were explored. In tests at 900°F indications were that the curves obtained by plotting the logarithm of stress-to-rupture against time-to-failure would be considerably flatter for glass-aluminum composites than for SAP, as would be expected if ultimate failure depended on fiber fracture rather than creep or flow of the metal. Permanent strain-hardening could not be induced in glass-aluminum composites as compared to SAP materials in which strain-hardening is one of the strengthening mechanisms operating.

The stress-strain diagrams of glass-metal composites were examined with the object of learning or explaining the role of each component in the strengthening mechanism. Matrix metals used were lead, zinc, and aluminum alloys; five of the nine aluminum alloys were variously heat treated. Marked differences were observed but none of such a nature as to explain behavior of the individual components. Stress-strain diagrams were of four general types:

        1. Initial yield followed by a straight line segment

        2. Continuously changing slope

        3. Typical of a metal

        4. Continuously but irregularly changing slope

Moduli computed from the curves varied widely at initial stressing. In a few cases moduli up to 25 million psi were indicated for composites which should not go over ten or eleven million psi. Moduli of three to seven million psi were computed for the straight line portion of 37 per cent of the curves (Type 1). If it is assumed that the modulus of the materials is an additive function of the area of the components, the modulus of the composites in the strained condition would be in the neighborhood of 2.2 million psi.

Breaks were of two types: one with a tangent modulus of more than one million psi and one with a tangent modulus of less than one half million psi. These results indicate that initial strength of the matrix does not appear to be the primary factor in determining strength of the composites and that shape of the stress-strain curves is affected more by heat treatment than by any other variable investigated.

Due to the large disparity in tensile strengths between vacuum injection cast glass-metal composites and handbook data for the matrix metal in the form of commercial wrought alloy bars, the effect of vacuum injection casting on strength was investigated.

Vacuum cast bars of the commercial alloy as received and diluted with one part 1100 aluminum to three of alloy were made in the same manner as glass-metal composites but omitting the glass fibers. The results of room temperature tests were not as decisive as desired due to loss of the undiluted commercial alloy bars which were not replaced. Compared on a cast basis, the indications were that dilution of the matrix alloy lowered its strength relatively little. The vacuum injection cast

glass-aluminum composites behaved similarly to the cast diluted alloy bars with the exception of reduced elongation. The major difference between cast and wrought alloy would appear to be one of basic structure. As previously reported the properties of wrought bars fade around 400°F whereas vacuum injection cast glass-aluminum composites continue strong to 700 - 900°F.

Attempts were made to relate the rate of fiber breakage in composites under stress to shapes of the stress-strain curves. Results showed that the fiber breaks in glass-lead bars could account for some of the change in the shape of the stress-strain curve. Results with glass-aluminum bars were not as positive. The rate of fiber breakage increased exponentially just prior to failure of the sample and bore no relation to shape of the curve. Work in this direction was discontinued.

Dr. Edward Saibel has composed a model system for glass-metal composites designed to explain and predict the properties of composites. His treatise, attached to this report as Appendix B, is similar to Dr. H. B. Whitehurst's treatise on the principles of fibrous reinforcements[1] but takes plasticity of the matrix into account. Experimental data fit both theories with some unexplained deviations.

---

[1]Appendix I, Tenth Quarterly Progress Report. Contract NOrd 15764, March 15, 1958, to June 15, 1958.

DISCUSSION

Development of Glass-Metal Composites
For Elevated Temperature Service

It was obvious that composites with strength in the range 1500 -
2000°F would require a glass of higher temperature endurance than "E"
glass. For this reason a method of drawing fibers from fused silica
rods was developed and placed into laboratory scale operation. Attempts
were made to coat the fused silica fibers with various metals at form-
ing. Aluminum was applied successfully but metals with melting points·
above aluminum (copper alloys) were not; oxide developed rapidly pre-
venting the metal from contacting the fiber. In those few cases where
continuous coating of high temperature alloys was achieved the fibers
were brittle and difficult to handle. A modification of the aluminum
coating technique will be necessary if metals which melt above 1500°F
are to be applied directly to fibers in the forming operation.

A few trials were made at vacuum injection casting molten metal
around the fibers, but copper and its alloys oxidize so rapidly that the
method was impractical. For this reason adaptations of conventional
powder metallurgy techniques were developed in which fibers coated with
metal powders were hot pressed in dies to form green compacts. A slurry
composed of metal particles suspended in a viscous liquid which served
as a heat fugitive binder was applied to the fibers in the forming opera-
tion. The particles adhered well enough to permit placing the fibers in
pressing dies. Dipping the fibers in ethylene glycol and rolling them in

metal powders was found to be an easier method for effecting the combination.

Hot pressed compacts of copper,. nickel, stainless steels, nickel-chromes and brass reinforced with fused silica fibers were produced. One bar was made with zirconium powder. Compacts containing over 50 per cent glass could not be made satisfactorily and the best glass percentages were relatively low, generally less than 10 per cent. With the exception of copper the bars all showed low green compact strength. This is not unusual for powdered metal compacts, but it does make handling more difficult. The use of 1100 aluminum precoats on the fibers resulted in denser, more easily handled compacts and was especially helpful for nickel compacts. Strengths of green compacts of copper (Table I) and nickel (Table II) were not exceptionally high but considering the low per cent of theoretical density achieved the results were quite favorable.

Sintering was not satisfactorily accomplished due to inadequacy of available furnaces in maintaining suitable protective atmospheres. Differential tnermal contraction between fiber and metal leading to severe internal stressing as the compacts cooled over a long temperature range was another problem encountered. The delamination observed was believed to be in part due to that cause and in part to oxidation. Possibly the differential shrinkage problem could be overcome by placing the bars under light to moderate pressure during the sintering and cooling steps.

At this time the necessary equipment for the high temperature work was not available at the Owens-Corning Fiberglas Corporation Research

Laboratories. For this reason it was recommended that the Navy Bureau
of Ordnance consider another contractor or subcontractor having adequate
facilities for investigating these high temperature composites. In the
meantime the Owens-Corning Fiberglas Corporation Research facilities
would be used to investigate the mechanism by which glass fibers and
metal matrixes interact to produce the properties exhibited by the
present composite materials.

Research Into Strength of Metal-Coated Glass Fibers and Methods of Improving the Coated Fiber Strength

For this phase of the work a faster, more sensitive method of
measuring the tensile strength of single fibers was required. A multi-
head tester was developed and constructed which was capable of testing
eight single fibers simultaneously and recording the results automat-
ically.[1] With an auxiliary jig (fork) for mounting fibers in the
tester, several hundred tests per day were quite possible. Tensile
strengths were computed from the recorded loading at break and the fiber
diameter as measured with a filar micrometer.

The first experiments were designed to check the correlation, if any,
between tensile strength and quality of the coating on the fibers. Assump-
tions had been that smooth, uniform, thin coatings yielded higher strengths.
Glasses RX78, "E" and "C" arranged in order of decreasing coatability were
coated with 1100 aluminum and the standard coating alloy (94 per cent Al -

---

[1] Twelfth Quarterly Progress Report. Contract NOrd 15764, September 15,
1958, to December 15, 1958.

5 per cent Zn - 1 per cent Cd). Within relatively narrow limits the coated fiber strength was a constant percentage of the virgin fiber strength for all three glasses, 20 - 24 per cent for 1100 aluminum and 17 - 23 per cent for the standard alloy.

These results indicated coating quality was not a controlling factor in coated fiber tensile strengths.

More recent work was done to determine what factors in the fiber forming and coating operation affect coating quality and fiber strength. The variables involved were:

1. Fiber forming temperature

2. Fiber pulling speed

3. Distance of metal coater from fiber-forming tip

4. Fiber diameter

5. Flow rate of metal onto the fiber

The results of the first tests were not very encouraging and it was decided to rerun the tests using statistical methods of changing these variables. (See Table III)

Before this was done it was decided to try improving the fiber forming and coating method to eliminate possible outside variations. This work involved forming as uniform a fiber as possible and producing as smooth a coating as possible. After a considerable expenditure of time, it was found that by using very high pulling speeds, such as 10,000 feet per minute and over, and controlling the flow of the metal by metering procedures that the above objectives could be accomplished. It was found, though, that the relative strength of these coated fibers was low

compared to other experimental results. The fiber strengths were 107,000 psi with a normal variation of $\pm$ 8,000 psi as compared to a normal overall average of 125,000 psi.

The experimentation changing the five parameters mentioned earlier was now reapplied on a statistical basis except that the flow of the metal was metered as best possible. The results of these experiments are shown in Table I and as can be seen other unrecognized variables are still influencing the experiments. This is best indicated by the fact that when a series of conditions were repeated in the experiment that the variations in results were as wide or wider than when changing the variables. There appeared to be no correlation between the variables and tensile strength, between the variables and fiber coating uniformity, and between fiber coating uniformity and tensile strength.

During this work it was found that fibers which were allowed to stand overnight showed a reduction in strength compared to fibers which were tested within a few hours of the time they were formed. This fact had also been noted in the Basic Physics Research Department and was accredited to the room humidity. A series of tests were designed in which coated fibers were tested in the virgin condition and metal-coated condition in atmospheres of 60 per cent and 5 per cent relative humidity. The virgin fibers showed an approximately 20 per cent increase in strength when tested in the low humidity condition. This was found to be true with aluminum-coated fibers also but not with lead-coated fibers. The results of this test were rather surprising in that it had always been assumed, based on microscopic examination, that the coating quality of aluminum-

coated fibers was superior to that of lead-coated fibers. No other explanation than coating discontinuity or porosity would appear to explain the differences between the two materials. This conclusion was further emphasized on applying wax coatings over the metal coatings. Although the wax did not eliminate change in tensile strength with changing humidity, the effect was greatly reduced. Aluminum wires tested as controls showed no change in strength with varying humidity.

Another more surprising indication was that several times forks would appear with exceptional strength of over 250,000 psi against an overall average of about 125,000 psi for coated fibers. These would seldom appear as single fibers on one fork, but rather as whole forks; and repeated checking into fiber diameter and the equipment failed to show any malfunction. All work to trace the reason for these exceptional strengths has ended in failure and at the present time no methods have been devised which will seemingly lead to an explanation.

A series of thermal expansion tests on metal-coated fibers was started and results of these tests are recorded in Figures 1, 2, 3, and 4. The reason for this work was an attempt to correlate experimental results with theory set forth in the treatise on "Thermal Expansion of Glass-Metal Composites" by R. B. Wiley.[1] Correlation was not possible either because the changes were smaller than experimental error or because the treatise did not cover enough of the variables involved.

---

[1]Eleventh Quarterly Progress Report. Contract NOrd 15764, June 15, 1958, to September 15, 1958.

Research Into Composites

As previously reported[1] work was done to check the possiblity that the reinforcing mechanisms operating in glass-metal composites might be the same as in dispersed oxide particle composites of which sintered aluminum powder (SAP) composites are typical. In summation the properties of glass-reinforced aluminum and SAP composites were found to be similar in many ways but due to the differences in interparticle spacing on which SAP theory is based it was concluded that the fibers did not act in the same way to modify the properties of the aluminum. Particle spacing in glass fiber reinforced aluminum is many times the minimum normally used in sintered aluminum powders and for similar properties there are differences of several hundredfold. This behavior was evident only at elevated temperatures and was intensified with increasing glass fiber content indicating dependence on presence of the glass in filament form. Additionally, the two materials differ in stress-rupture and cold working properties. Stress-to-rupture versus time-to-failure curves for glass-aluminum composites look to be flatter than those for SAP indicating again dependence on fibers rather than discrete particles and metal flow. Permanent strain-hardening could not be induced in glass-aluminum composites but is known to operate in SAP materials as one of the strengthening mechanisms. Cold working glass-aluminum composites either by extrusion or rolling is difficult at best; severe cracking is encountered with glass

---

[1]Tenth Quarterly Progress Report. Contract NOrd 15764, March 15, 1958, to June 15, 1958.

contents much over 10 per cent when these operations are done in the
normal manner. In general no increase in strength after cold working
and annealing was noted and for those samples that could be rolled with
great difficulty the strength actually decreased. This behavior indicated
a distinctly different mechanism of reinforcement for glass-fiber metal
composites.

A better understanding of the nature of glass-metal composites was
the primary reason for studying changes in stress-strain curves caused
by varying the matrix metal. Correlation of rate of fiber breakage in
composites under stress with shape of the stress-strain curves was
attempted by recording the sound of the breaking fibers. The objective
in both cases was to determine effect of the fibers on the matrix mate-
rials. Preliminary results have been reported.[1]

Results with glass-fiber lead composites indicated that the fiber
was the factor controlling the shape of the stress-strain curve. As the
rate of fiber breakage increased, the shape of the curve changed at
approximately the same rate.

While all the stress-strain curves are not shown in this report,
three of them illustrate the variations caused by changing the matrix
metal. Figure 5 presents a comparison of stress-strain curves for
glass-fiber lead, glass-fiber aluminum, and glass-fiber zinc composites.
The composites were prepared by vacuum injection casting and contain

---

[1]Twelfth Quarterly Progress Report. Contract NOrd 15764, September 15,
1958, to December 15, 1958.

approximately 20 per cent glass fibers by volume. Tests were conducted at room temperature.

Figure 6 shows the relationships between three aluminum matrix composites vacuum injection cast with 20 per cent "E" glass fibers by volume. The first curve is for 1100 aluminum. The second curve is for 2014 aluminum solutioned and aged after casting. The third curve is for 4032 aluminum also with solution and aging heat treatment after casting. These three curves show the difference that alloys can make in composites.

Figure 7 presents four curves showing the effects of various types of heat treatment on a composite of 2014 aluminum vacuum injection cast with 20 per cent "E" glass fibers by volume. The curves represent the as cast, annealed, solutioned, and solutioned and aged conditions of heat treatment. These are average curves typical of results obtained and do not represent any one composite.

The work on the stress-strain sound recording of aluminum composites proceeded very satisfactorily using the modified sound recording system previously described.[1] Figures 8 and 9 present typical stress-strain curves with representative fiber breakage rate curves for aluminum composite materials. Figure 8 presents a glass-aluminum composite in which the matrix material is 1100 aluminum and Figure 9 presents a composite in which the matrix material is 2014 aluminum after solutioning and aging. As can be seen from these curves, the shape of the stress-strain curve cannot be readily predicted from the change in the rate of fiber breakage.

---

[1]Twelfth Quarterly Progress Report. Contract NOrd 15764, September 15, 1958, to December 15, 1958.

In fact, due to the almost entirely exponential shape of the fiber breakage curve, the only thing that can be discerned is that when one is checking the sound of fiber breakage during a stressing operation approximately five to ten seconds' warning is given as to the time at which the composite will break. Work with the stress-strain sound experiment, therefore, has been discontinued at the present time.

Due to the wide difference in the ultimate tensile strengths found experimentally for glass-aluminum composites and the ultimate strengths as published for the commercial alloys, it was decided to see what effect the casting system used in producing composites might have on the strength of the commercial alloys. Rods of the various alloys were vacuum cast in the same manner as for composites but with fiber omitted. Also, due to the fact that glass fibers normally are coated with 1100 aluminum, bars were made of the commercial alloy diluted with 25 per cent 1100 aluminum. This percentage is about the same dilution of the matrix alloy as in typical vacuum injection cast composites. The experiment turned out not to be as decisive as desired due to loss of the undiluted alloy bars before testing which were not replaced after the flood. Tensile strengths of composites are compared with strengths of diluted alloy bars and handbook data in Table IV. Any conclusions drawn from these data may be labeled speculative and based on slim evidence. However, the data tend to show that dilution of the matrix with casting alloys lowers its strength relatively little. The composites have strengths like the diluted alloy bars indicating the addition of fibers did not weaken them. It is inferred that the main difference between cast and wrought commercial alloy bars

arises from differences in basic metal structure in the two conditions.
This difference is erased at temperatures above 400°F for commercial
alloys versus composites which continue strong to 700 - 900°F.

To check R. B. Wiley's treatise "Thermal Expansion of Glass-Metal
Composite Materials,"[1] checks were made on the thermal expansion of
glass-metal composites. In particular lead, zinc, and aluminum compos-
ites were studied. The test apparatus did not function properly for
the higher temperatures required in testing the glass-aluminum compos-
ites, but curves were obtained for the lead and zinc materials and data
on 2014 aluminum-glass composites were available from earlier trials.
These are shown in Figure 10. But after re-examination of the experi-
mental apparatus, it is felt that while the curves are valid, they were
not under fine enough control to either prove or disprove the work done
by R. B. Wiley. Future work in this area is still planned.

Theoretical Studies of Glass-Metal Composites

In the 10th Quarterly Progress Report, Dr. H. B. Whitehurst presented
a paper in which he used glass reinforced plastic composites as a model
to describe glass-metal composites. The main consideration in this trea-
tise is that both the composite components are deformed elastically under
stress. Dr. E. Saibel of Rensselaer Polytechnic Institute has since fol-
lowed this same line of reasoning but has utilized known experimental and

---

[1]Eleventh Quarterly Progress Report. Contract NOrd 15764, June 15,
1958, to September 15, 1958.

theoretical work on metals to devise a set of experimental curves for glass-aluminum composites allowing for the plastic deformation of metals under stress. This treatise is found in Appendix B. Both of these theoretical works seem to fit fairly closely to experimental data, but there are deviations which cannot be explained exactly. Whether it is due to the assumptions that had to be made or whether it is due to an experimental error or by coincidence that the curves happened to follow those of the theories is not understood. A conclusive test to discern the facts has not been found at the present time.

FUTURE PLANS

Work in the next period will follow the same pattern of trying to discern what the effects of the glass and metal are in producing the unique set of properties found for the composite materials. Most of this work will be an extension of the present work and will be divided into two classes.

One will be concerned with attempts to prove validity and applicability of any of the three theories advanced, i.e.; R. B. Wiley's treatise, Dr. H. B. Whitehurst's theory, and Dr. E. Saibel's theory.

The other area of interest is concerned with prosecuting studies on both aluminum-coated fibers and composites at high temperatures. Specifically, fiber strengths and stress-strain behavior of various composites at elevated temperatures will be examined. Stress-strain behavior of composites with low percentages of glass is of particular interest.

APPENDIX A

TABLES AND FIGURES

TABLE I

UNSINTERED FUSED SILICA-COPPER COMPOSITES
TENSILE STRENGTH

Fused Silica Fibers. 0.0005 - 0.001 Inch Diameter.
3% by Wt. Oriented Parallel
Hot Pressed at 900°F & 16.6 tons/sq.in. Not Sintered.

Temperature °F	Tensile Strength Psi	Elongation %
Room	46,900	3.9
	32,000	—
	4,420	0
	14,050	0
500	10,500	—
	22,500	1.56
1100	4,043	—
	3,800	—
	1,900	—
1500	484	—
	402	6.25
	402	--
Control	No Glass Fibers	
Room	27,500	0.78

TABLE II

UNSINTERED FUSED SILICA-ALUMINUM-NICKEL COMPOSITES
TENSILE STRENGTH

Fused Silica Fibers. 0.00075 - 0.0012 Inch Diameter.
Precoated with 1100 Aluminum. Oriented Parallel.
Hot Pressed at 1100°F & 14 tons/sq.in. Unsintered.
Tested at Room Temperature

Composition - % by Wt.			Tensile Strength Psi	Average Tensile Strength Psi
Fiber	Al	Ni		
5	5	90	3323 4075	3699
10	10	80	6947 9542 6491	7660
*16.66	16.66	66.66	10637 11412 8113	10054

*Specific Gravity: Theoretical 4.99
                     Actual   4.42
                     89.1% of Theoretical

TABLE III

EXPLORATION OF VARIABLES
CONTROLLING TENSILE STRENGTH AND COATING SMOOTHNESS
OF ALUMINUM COATED "E" GLASS FIBERS

Single Fiber Data on 24 or More "E" Glass Fibers
Coated With 1100 Aluminum Metal

Bushing Temp. °F	Pulling Speed Ft/Min	Dist. of Coater From Forming Tip—In.	% Metal In Head In Coater	Bare Fiber Dia. In.x10⁻⁵	Coated Fiber Dia.Min. In.x10⁻⁵	Coated Fiber Dia.Max. In.x10⁻⁵	Ave. Coated Fiber Dia. In.x10⁻⁵	Ave. Thickness Coating In.x10⁻⁵	Fiber Weight (Timed Runs) Grams Bare	Coated	% Metal Applied	Tensile Strength x 10³psi
2400	7,000	1.5	100	30	36	—	36	3	0.254	—	—	125
2400	4,300	1.5	100	38	48	60	54	8	0.271	0.504	46	156
2400	2,700	1.5	100	53	74	89	82	14	0.284	0.512	45	140
2450	2,890	1.5	100	58	64	78	71	6	0.357	0.633	43	125
2450	2,160	1.5	100	64	70	95	82	9	0.357	0.577	38	124
2450	1,260	1.5	100	83	96	109	103	10	0.350	0.450	22	94
2500	1,260	1.5	100	88	100	111	106	17	0.387	0.570	26	80
2500	540	1.5	100	136	177	177	177	20	0.440	0.701	37	73
2400	7,000	1.5	100	32	36	62	49	9	0.297	0.778	62	165
2450	2,880	1.5	100	59	63	105	84	13	0.389	0.761	49	97
2500	1,260	1.5	100	99	102	132	117	9	0.493	0.780	37	83
2450	2,890	1.5	50	53	60	80	70	9	0.324	0.787	59	130
2500	1,260	1.5	50	98	127	151	139	20	0.479	0.652	27	84
2400	7,000	1.5	50	33	41	41	41	2	0.296	—	—	97
2500	1,260	1.5	12	89	100	123	111	11	0.394	0.555	25	—
2450	2,890	1.5	12	55	66	101	84	14	0.362	0.554	35	117
2400	7,000	1.5	12	34	37	55	46	6	0.301	—	—	121
2425	2,500	2.5	100	59	63	122	93	24	0.344	0.594	42	119
2475	5,500	2.5	100	45	67	85	76	16	0.413	1.246	67	126
2550	4,000	2.0	100	51	61	77	69	9	0.424	0.680	37	123

TABLE III (Continued)
Page 2

Bushing Temp. °F	Pulling Speed Ft/Min	Dist. of Coater From Forming Tip--In.	%Metal Head In Coater	Bare Fiber Dia. In.x10^-5	Coated Fiber Dia.Min. In.x10^-5	Coated Fiber Dia.Max. In.x10^-5	Ave. Coated Fiber Dia. In.x10^-5	Ave. Thickness Coating In.x10^-5	Fiber Weight (Timed Runs) Grams Bare	Fiber Weight (Timed Runs) Grams Coated	% Metal Applied	Tensile Strength x 10^3 psi
2425	5,500	2.5	100	38	58	63	61	11	0.326	0.427	35	175
2400	4,000	2.0	100	42	56	69	63	9	0.242	0.726	60	145
2475	2,500	1.5	100	63	81	92	86	11	0.421	0.815	48	103
2475	5,500	1.5	100	40	47	56	51	6	0.353	0.600	41	140
2450	4,000	2.5	100	45	54	120	87	21	0.350	1.160	70	148
2425	2,550	1.5	100	63	51	99	75	6	0.329	0.700	53	113
2475	2,000	2.5	100	61	68	157	113	26	0.387	1.490	74	114
2475	5,500	2.0	100	46	44	64	54	4	0.297	0.765	61	97
2450	4,000	2.0	100	39	52	75	64	12	0.368	0.657	44	192
2425	5,500	2.0	100	39	61	68	65	12	0.337	0.896	52	157
2450	7,000	2.0	100	33	41	63	52	9	0.341	0.838	59	119
2425	2,500	2.5	100	58	68	97	83	12	0.348	0.681	49	117
2450	1,000	2.0	100	94	106	132	119	12	0.333	0.453	27	76
2450	4,000	2.0	100	53	67	104	86	17	0.460	0.712	35	163
2425	2,500	2.0	100	53	57	92	75	11	0.316	0.448	30	114
2450	4,000	2.0	100	48	52	111	82	17	0.372	0.769	52	152
2475	2,500	1.5	100	66	68	98	83	8	0.435	0.650	33	126
2425	5,500	2.5	100	42	64	53	57	6	0.366	0.771	53	135
2475	5,500	2.5	100	36	37	50	44	9	0.337	0.533	37	132
2475	2,500	1.5	100	63	76	124	100	16	0.422	1.237	66	115
2475	5,500	1.5	100	42	47	68	59	8	0.411	0.890	54	146
2475	2,500	1.5	100	52	65	114	90	14	0.392	0.646	39	115
2450	4,000	1.0	100	44	56	64	60	8	0.320	0.404	21	131
2450	4,000	3.0	100	47	60	61	60	6	0.367	0.637	42	157
2425	5,500	2.5	100	39	47	106	77	18	0.336	1.668	80	125

TABLE III (Continued)
Page 3

Bushing Temp. °F	Pulling Speed Ft./Min	Dist. of Coater From Forming Tip--In.	% Metal Head In Coater	Bare Fiber Dia. In.x10⁻⁵	Coated Fiber Dia.Min. In.x10⁻⁵	Coated Fiber Dia.Max. In.x10⁻⁵	Ave. Coated Fiber Dia. In.x10⁻⁵	Ave. Thickness Coating In.x10⁻⁵	Fiber Weight (Timed Runs) Grams Bare	Coated	% Metal Applied	Tensile Strength x10³ psi
2450	4,000	2.0	100	47	58	98	78	15	0.364	0.952	61	140
2425	2,500	2.5	100	54	59	87	73	9	0.303	1.166	74	135
2475	2,500	2.5	100	64	65	76	70	3	0.404	0.679	49	132
2425	5,500	1.5	100	35	39	83	61	12	0.288	1.016	72	173
2450	4,000	2.0	100	47	58	59	58	5	0.357	0.527	32	127
2425	2,500	1.5	100	57	61	116	88	15	0.337	0.748	55	58
2475	5,500	2.5	100	41	47	72	59	10	0.356	0.776	54	157
2475	5,500	1.5	100	41	47	54	51	5	0.369	0.562	34	157
2425	5,500	1.5	100	41	49	53	51	5	0.346	0.976	65	127
2450	4,000	1.5	100	46	52	93	72	3	0.378	0.700	46	191
2450	4,000	2.0	100	48	62	66	64	8	0.372	0.635	41	122
2425	5,500	2.5	100	40	60	60	60	10	0.330	0.776	57	162
2475	5,500	2.5	100	44	49	58	53	5	0.430	0.610	29	119
2450	4,000	2.5	100	48	65	70	68	10	0.384	0.715	46	128
2475	2,500	2.5	100	63	75	82	78	7	0.412	0.670	24	134
2475	2,500	1.5	100	64	69	109	89	12	0.407	0.736	45	74
2475	2,500	1.5	100	42	48	72	60	9	0.384	0.888	51	105
2450	4,000	2.0	100	50	51	81	66	8	0.381	0.761	50	129
2425	2,500	1.5	100	54	59	106	83	14	0.311	0.661	53	127
2425	2,500	2.5	100	59	66	67	66	3	0.339	0.611	45	140

TABLE III (Continued)
Page 4

Reruns of Earlier Data
Six Fibers or More Tested

Bushing Temp. °F	Pulling Speed Ft./Min.	Dist. of Coater From Forming Tip--In.	% Metal In Head In Coater	Bare Fiber Dia. In.x10^-5	Coated Fiber Dia.Min. In.x10^-5	Coated Fiber Dia.Max. In.x10^-5	Ave. Coated Fiber Dia. In.x10^-5	Ave. Thickness Coating In.x10^-5	Fiber Weight (Timed Runs) Grams Bare	Coated	% Metal Applied	Tensile Strength x10^3 psi
2300	2,700	1.0	100	41	51	73	62	11	0.115	0.248	34	117
2400	4,000	1.0	100	40	52	64	58	9	0.260	0.453	43	140
2500	7,000	1.0	100	34	46	70	58	12	0.370	0.668	45	122
2300	2,700	1.5	100	43	46	85	66	11	0.212	0.628	66	83
2400	4,000	1.5	100	38	56	65	61	11	0.268	0.557	52	136
2500	7,000	1.5	100	39	41	56	48	11	0.424	0.792	53	128
NO RUN - Glass would not coat												
2400	4,000	2.0	100	40	49	59	54	7	0.254	0.481	48	106
2500	7,000	2.0	100	37	41	60	50	7	0.432	1.066	60	123
NO RUN - Glass would not coat												
2400	4,000	2.5	100	40	43	91	67	12	0.273	0.580	47	140
2500	7,000	2.5	100	38	42	77	60	10	0.401	1.128	64	117
2300	2,700	3.0	100	42	50	94	72	15	0.168	0.439	63	175
2400	4,000	3.0	100	39	51	85	68	14	0.265	0.727	63	240
2500	7,000	3.0	100	36	45	57	51	13	0.411	0.739	44	158
NO RUN - Glass would not coat												
NO RUN - Glass would not coat												
2500	7,000	4.0	100	46	56	64	60	7	0.415	0.832	50	80

TABLE III. (Concluded)
Page 5

Bushing Temp. °F	Pulling Speed Ft./Min.	Dist. of Coater From Forming Tip—In.	% Metal Head In Coater	Bare Fiber Dia. In.x10^-5	Coated Fiber Dia.Min. In.x10^-5	Coated Fiber Dia.Max. In.x10^-5	Ave. Coated Fiber Dia. In.x10^-5	Ave. Thickness Coating In.x10^-5	Fiber Weight (Timed Runs) Grams Bare	Coated	% Metal Applied	Tensile Strength x 10^3 psi
2500	7,000	1.0	100	40	41	65	53	6	0.461	0.934	56	123*
2500	7,000	1.0	100	42	44	63	54	6	0.396	1.030	62	96
2500	7,000	1.0	100	42	49	68	58	8	0.485	1.721	58	128
2500	7,000	1.0	100	42	46	68	57	5	0.349	0.943	62	128**
2500	7,000	1.0	100	40	42	68	55	8	0.317	0.975	67	131
2500	7,000	1.0	100	37	42	72	57	10	0.375	1.042	64	200

* One small cone on coater lip
** Double cone on coater lip
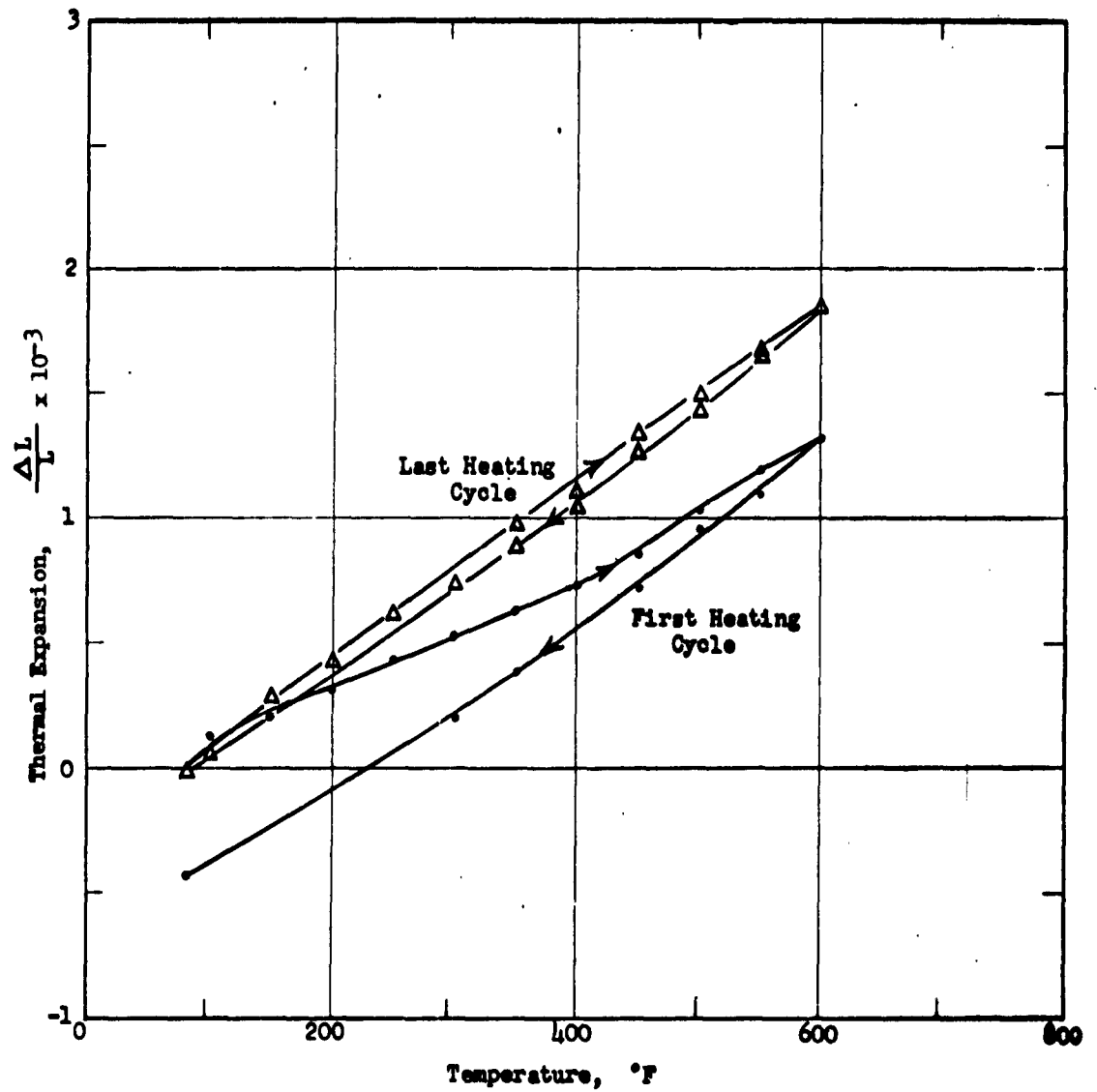
Figure 1 - Thermal Expansion of Single Fibers.
Lead Alloy (1% Zn, 1-1/2% Cd) Coated "E" Glass
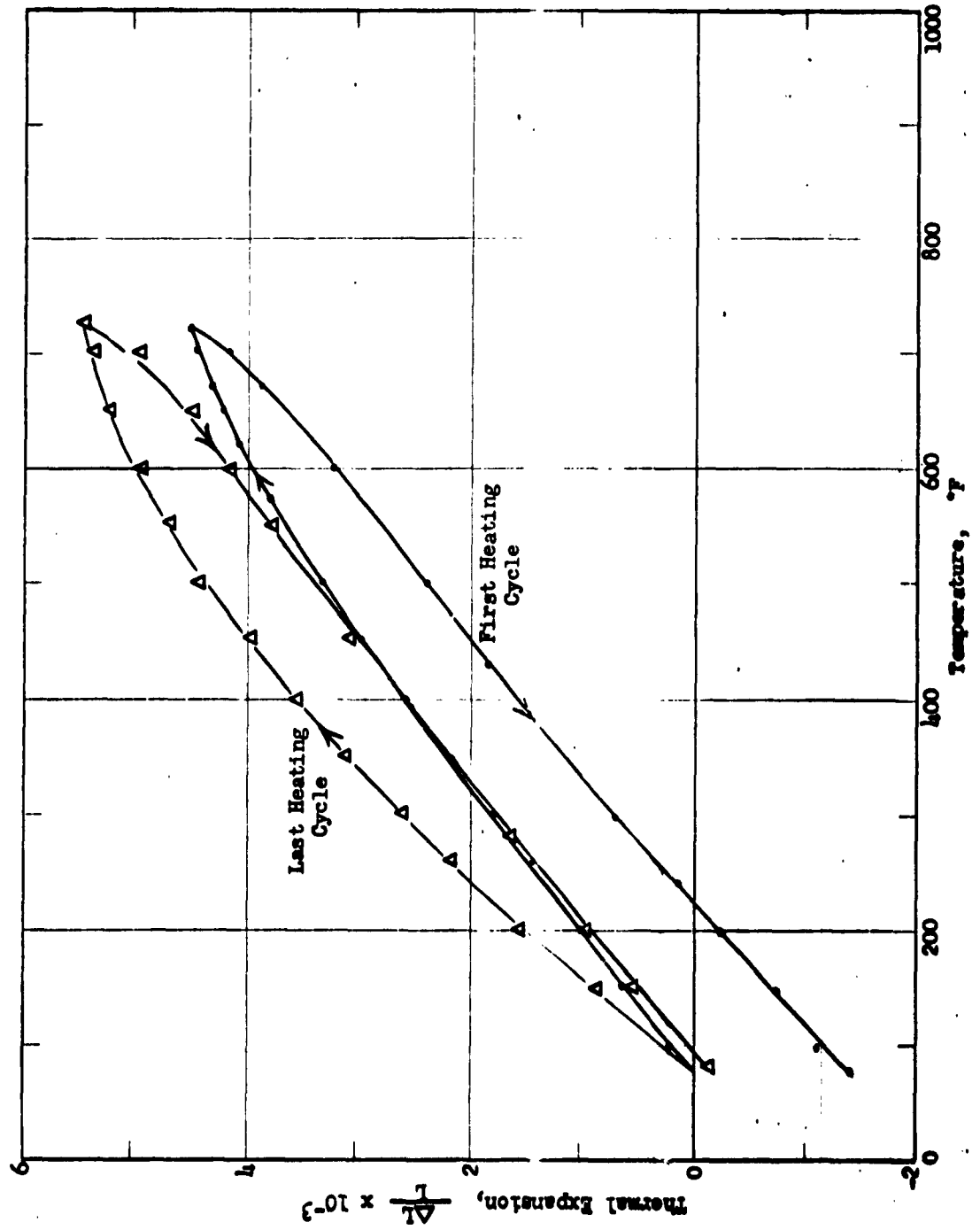
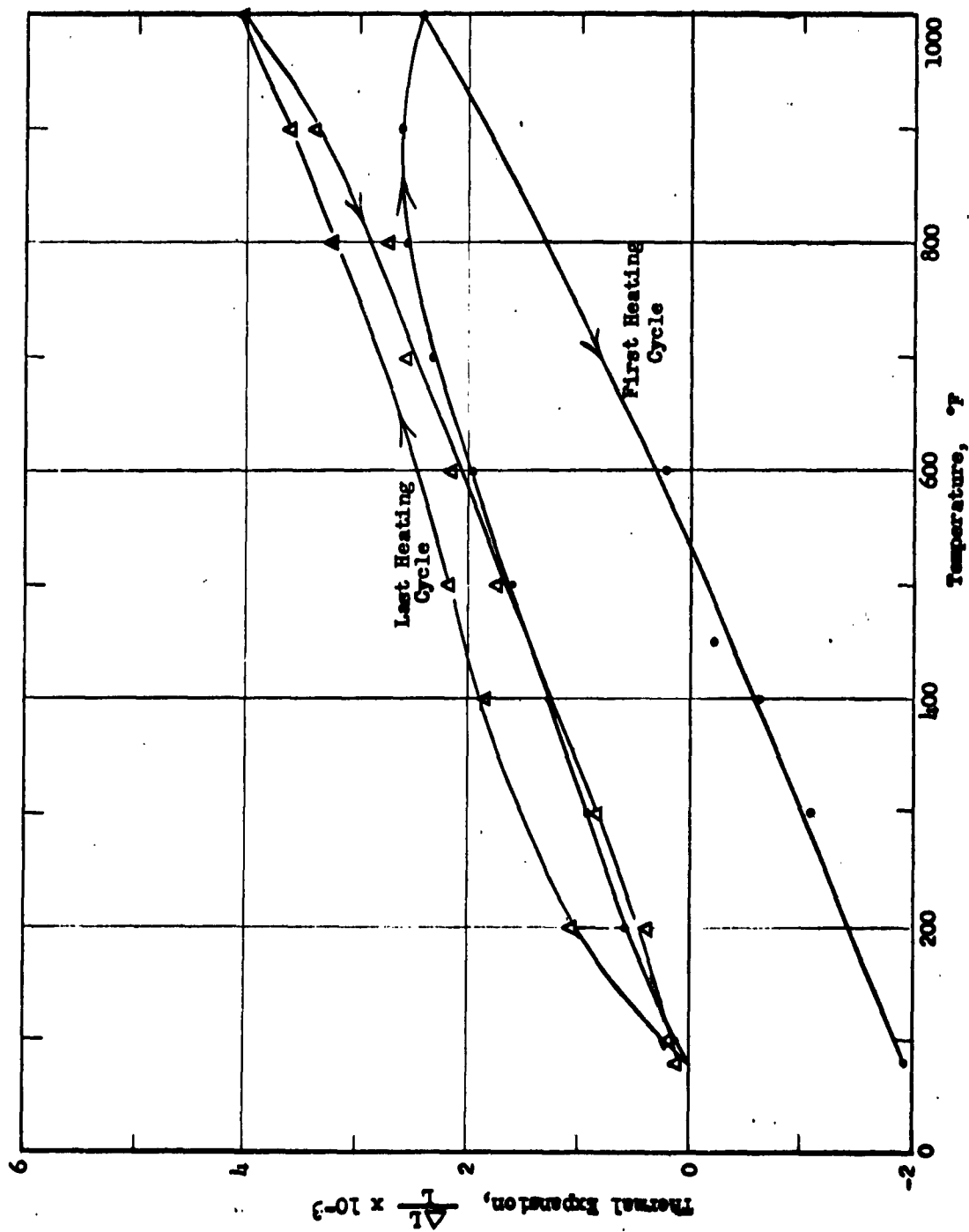Figure 2 - Thermal Expansion of Single Fibers - Zinc Coated "g" Glass

Figure 3 - Thermal Expansion of Single Fibers - Aluminum Alloy (5% Zn, 1% Cd) Coated "E" Glass
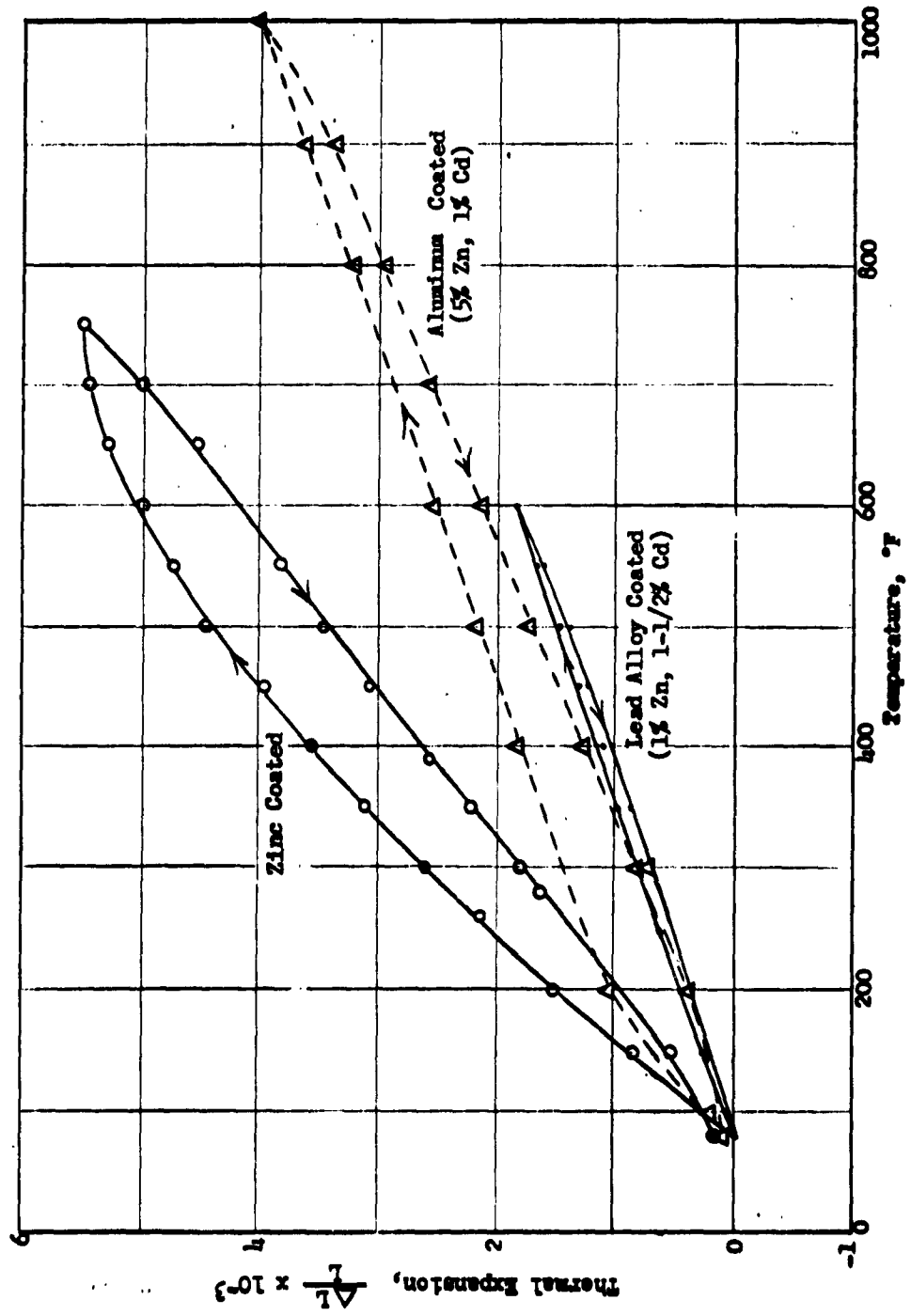
Figure 4 - Thermal Expansion of Coated "E" Glass Single Fibers after Repeated Heatings
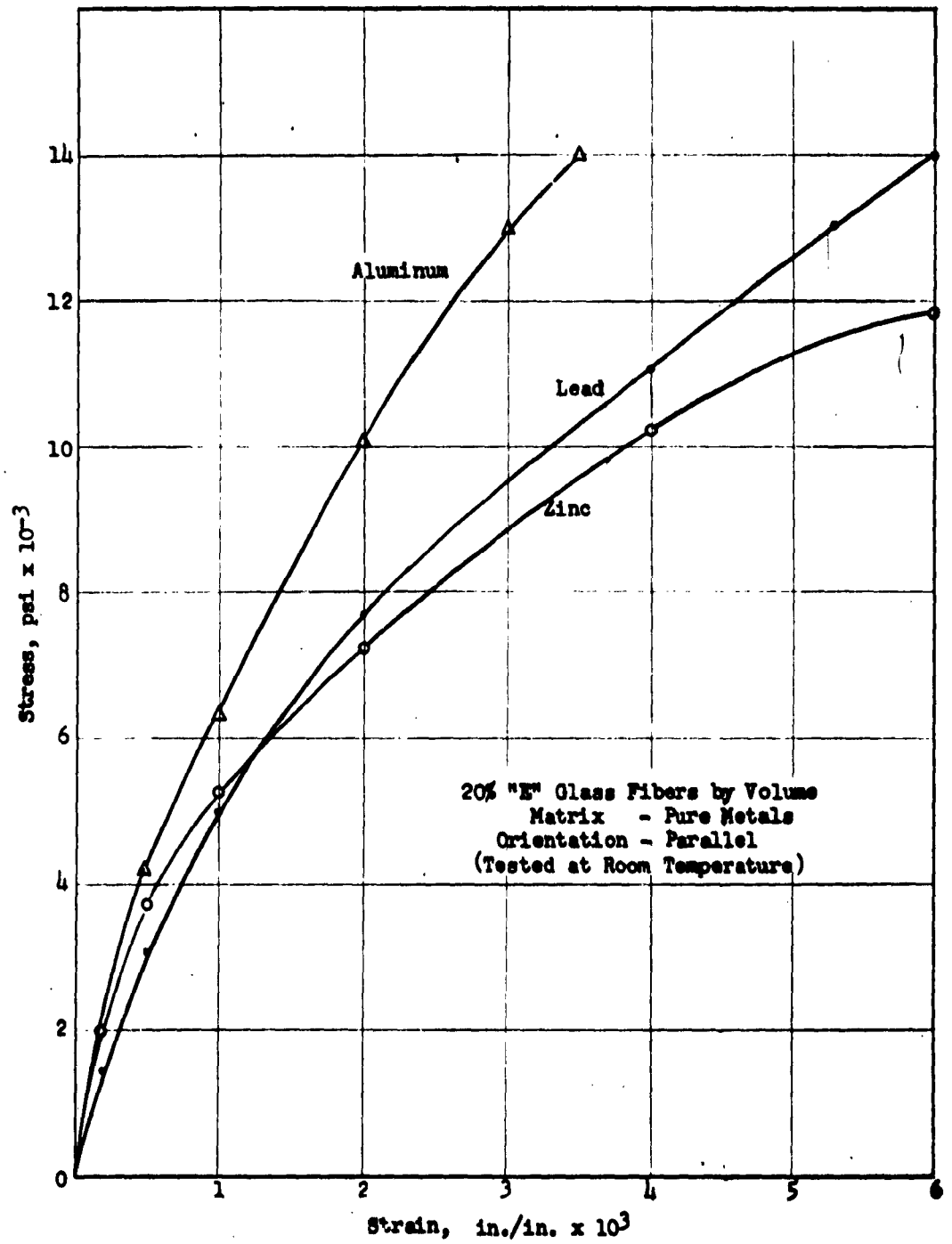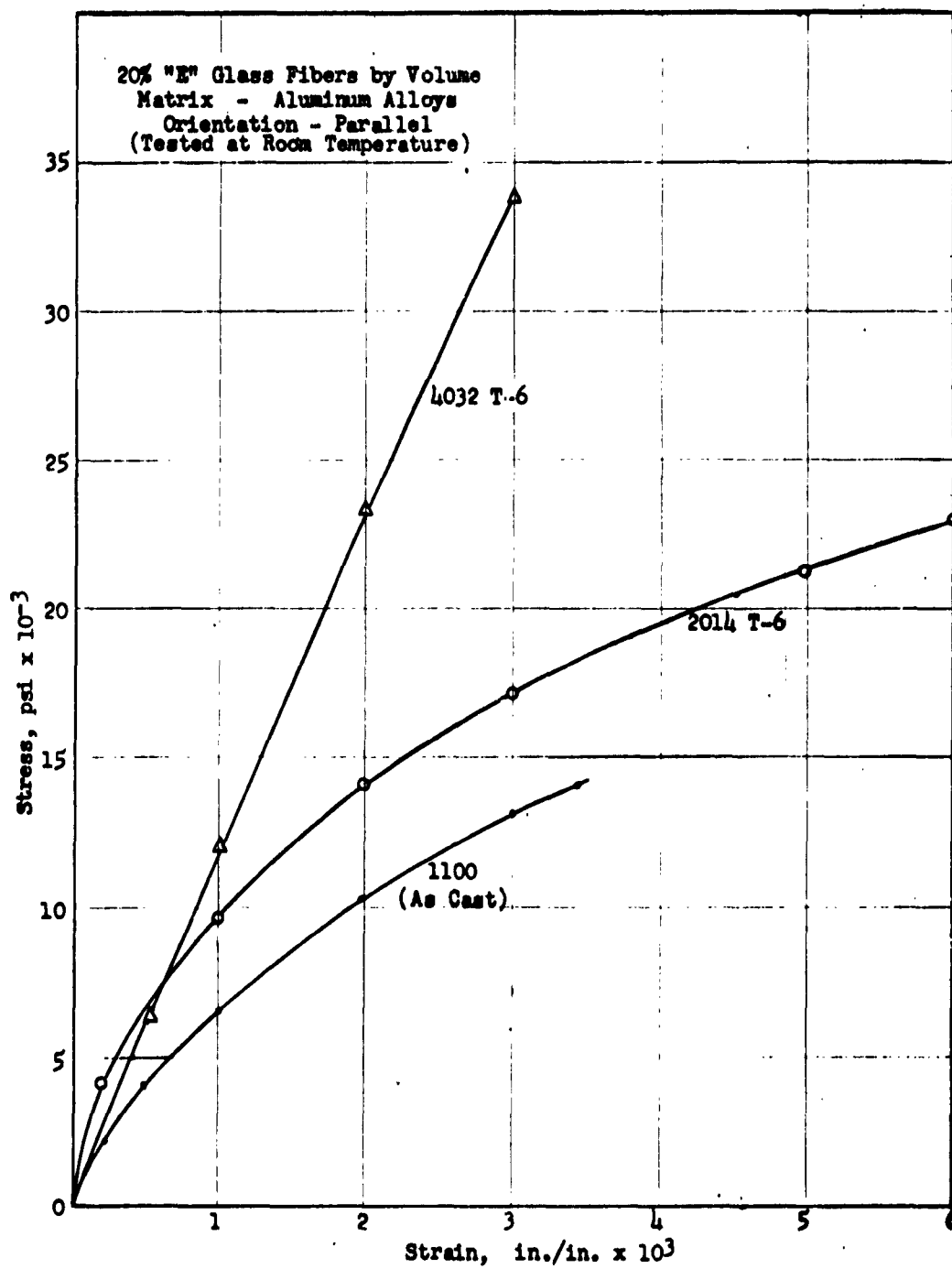
Figure 5 - Tensile Stress-Strain Curves
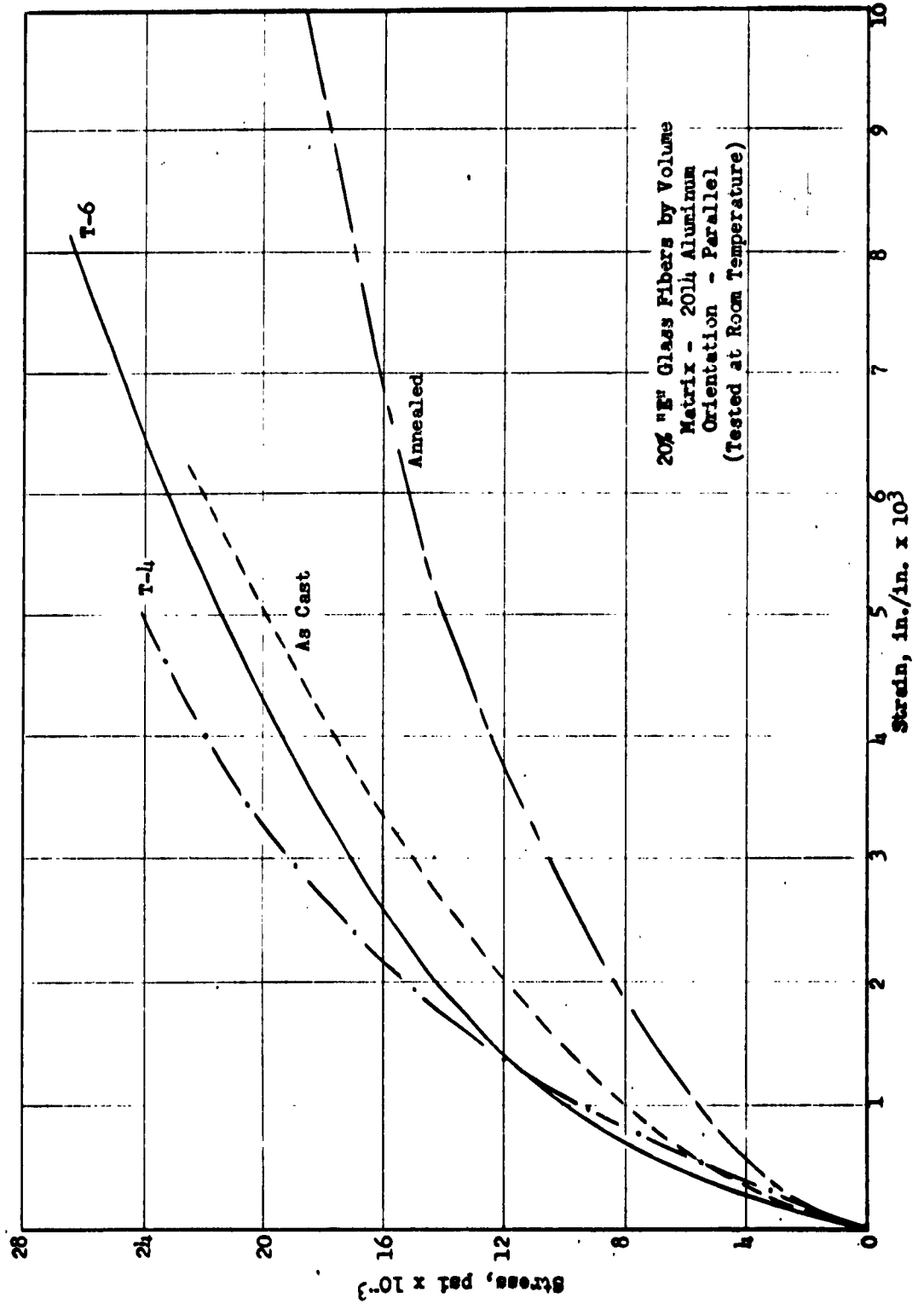
Figure 6 - Tensile Stress-Strain Curves

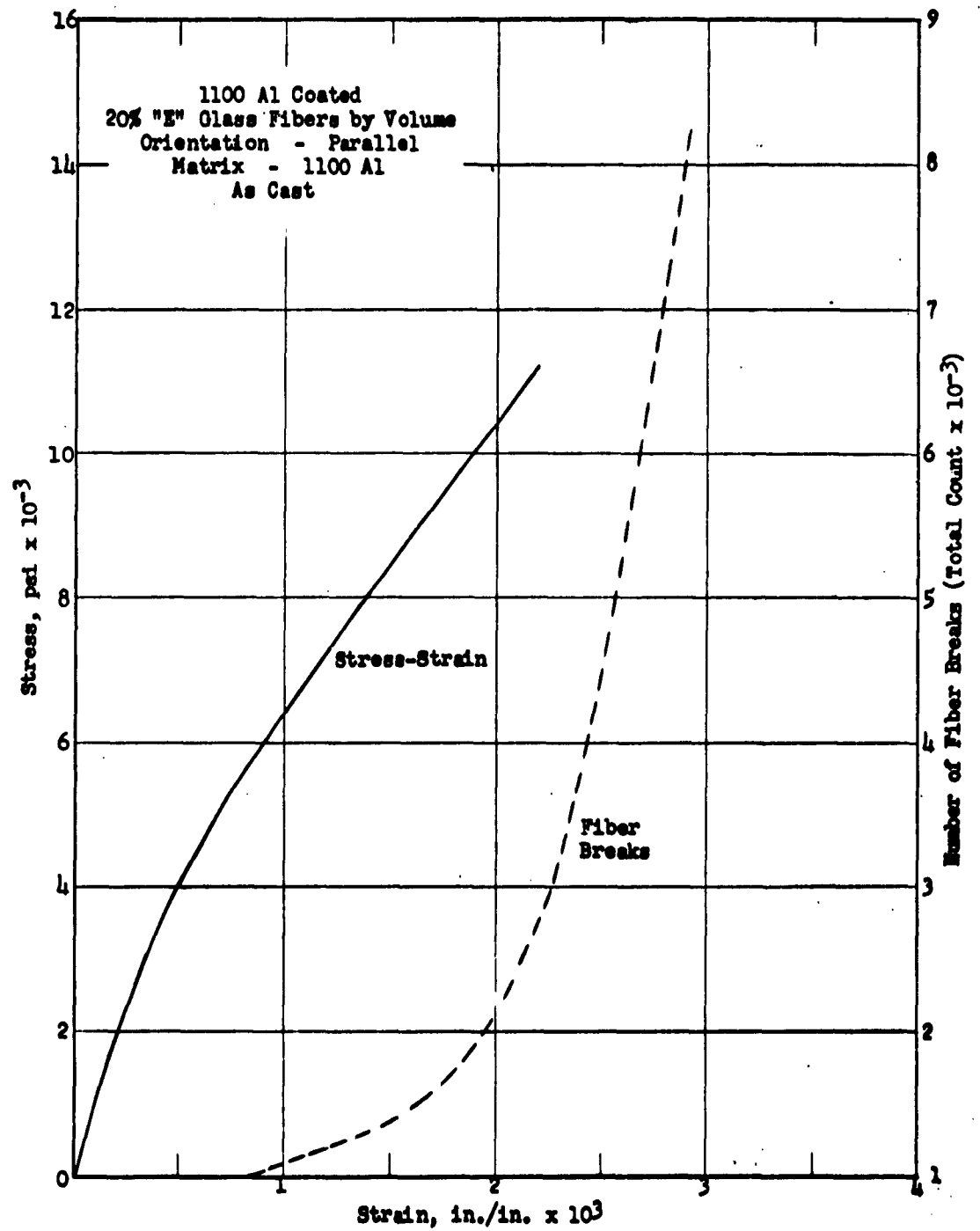Figure 7 - Stress-Strain Differences with Heat Treatment

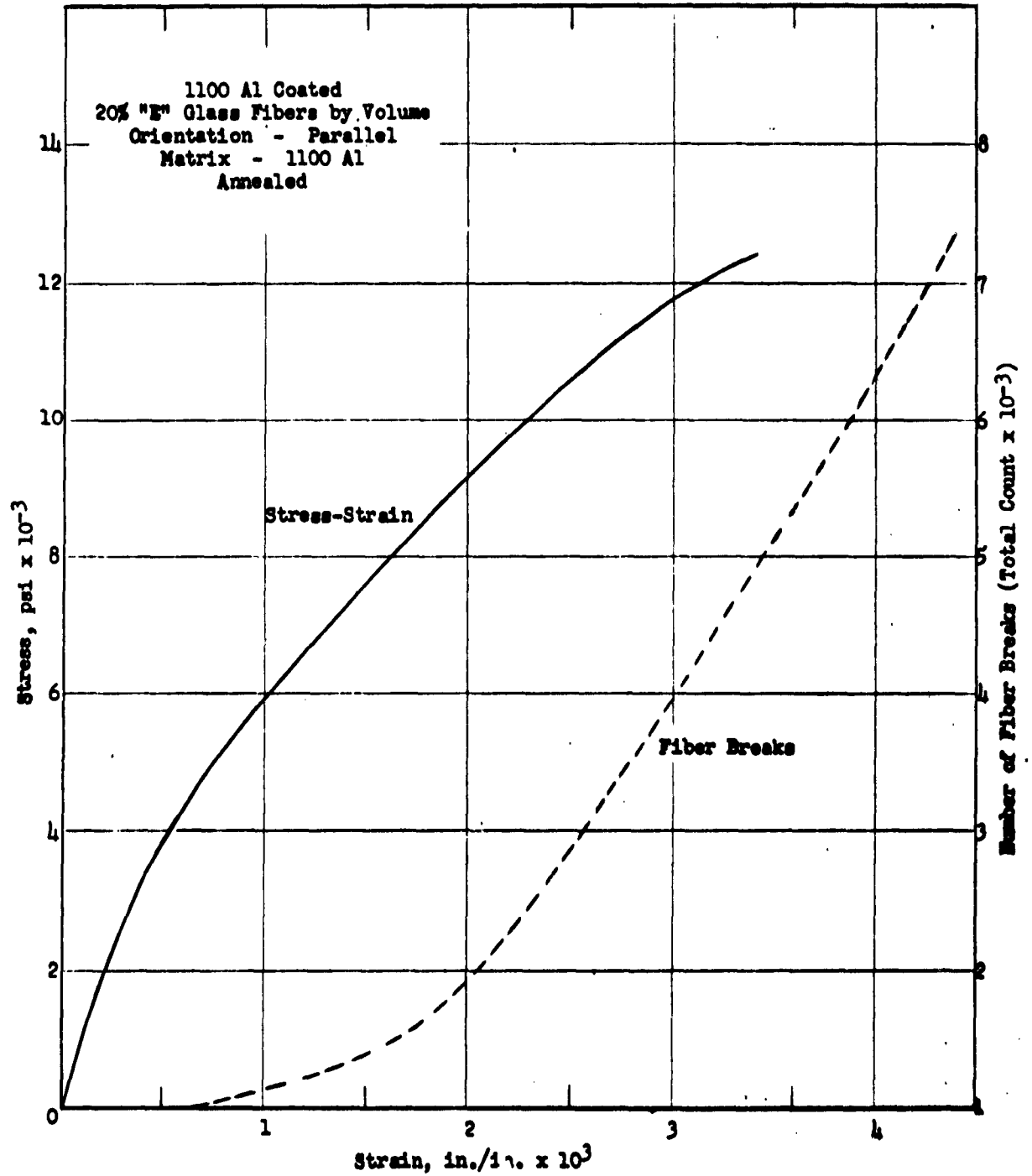Figure 8a - Tensile Stress-Strain vs Fiber Breaks
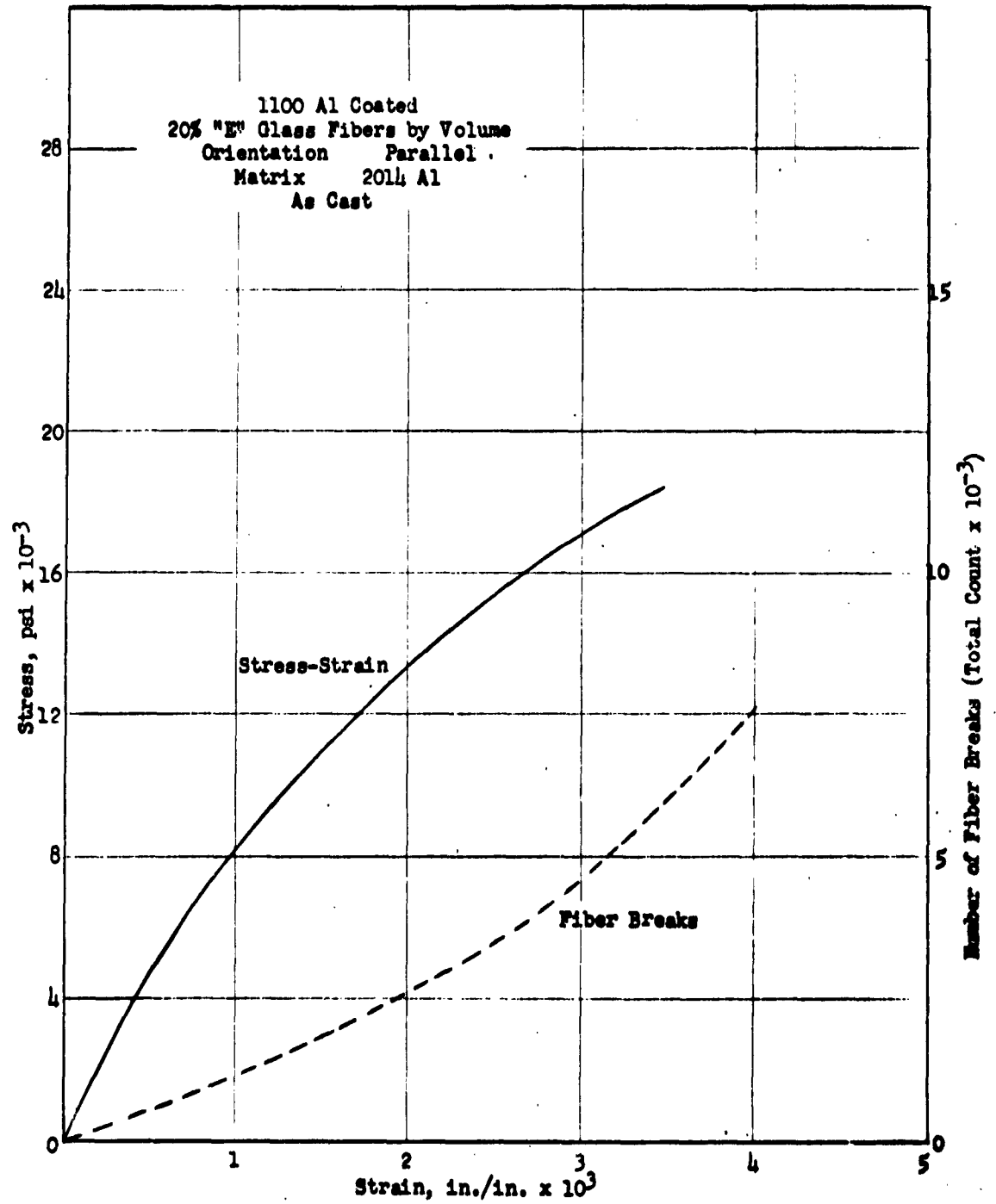
Figure 6b - Tensile Stress-Strain vs Fiber Breaks

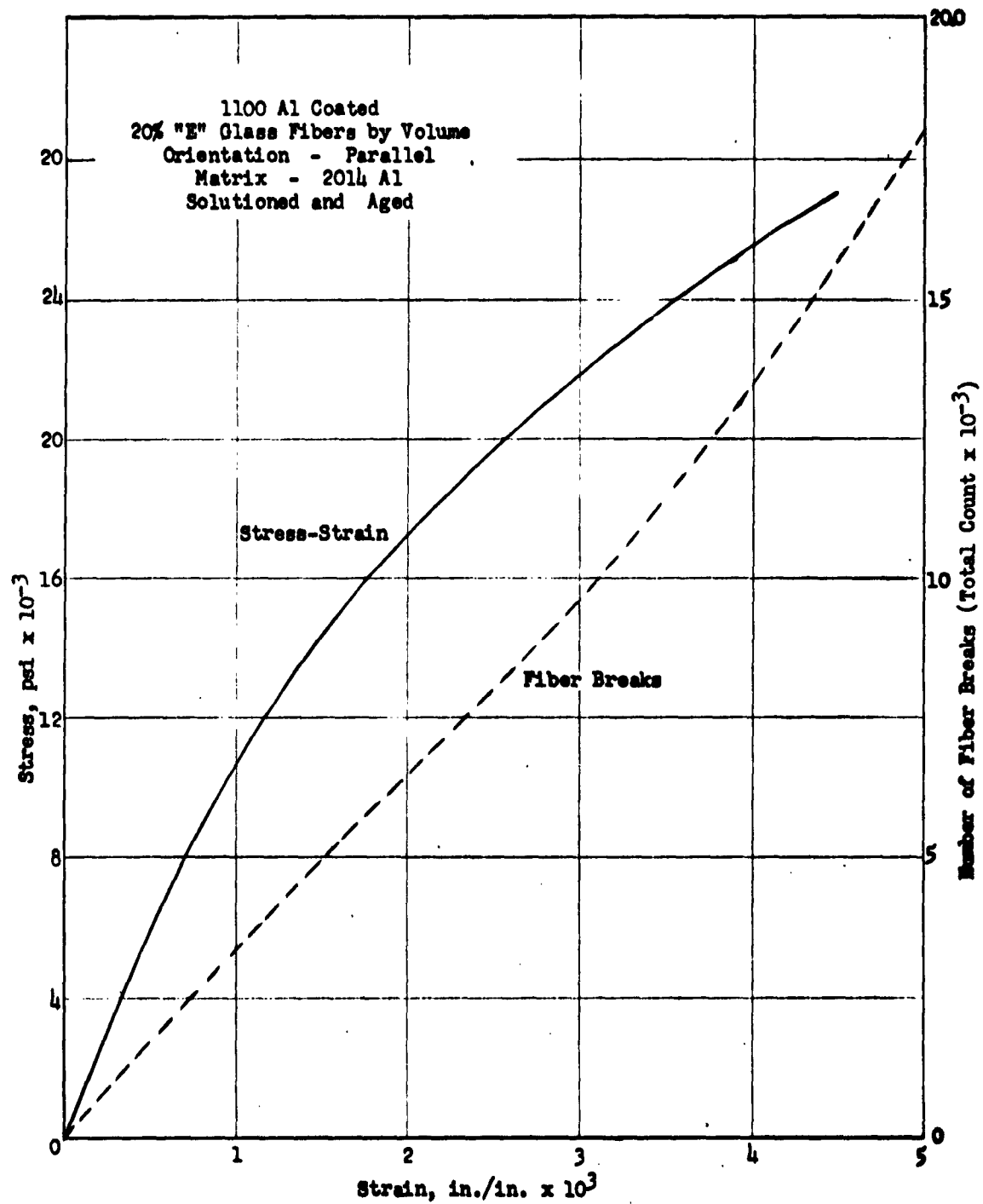Figure 9a - Tensile Stress-Strain vs Fiber Breaks

Figure 9b - Tensile Stress-Strain vs Fiber Breaks

TABLE IV

TENSILE STRENGTH COMPARISONS

Composites - 20% by Volume "E" Glass
Parallel Oriented 1100 Aluminum Coated
with Aluminum Matrixes

Tested at Room Temperature

Alloy	Ultimate Tensile Strength psi x 10^{-3}			Elongation %		
	As Cast	An-nealed	Solution & Aged	As Cast	An-nealed	Solution & Aged
1100 Aluminum						
Composite	14.5	14.1	—	0.32	0.34	—
Laboratory Casting*	9.1	5.2	—	—	—	—
Commercial (Wrought)**	18.0	13.0	—	20.0	45.0	—
2014 Aluminum						
Composite	23.2	18.5	27.0	0.6	1.0	0.8
Laboratory Casting*	14.7	—	24.5	—	—	—
Commercial (Wrought)**	—	25.0	68.0	—	21.0	10.0
4032 Aluminum						
Composite	21.3	—	33.1	0.8	—	0.4
Laboratory Casting*	17.9	—	29.4	—	—	0.4
Commercial (Wrought)**	—	—	55.0	—	—	9.0
5056 Aluminum						
Composite	18.8	17.2	—	0.7	0.4	—
Laboratory Casting*	19.4	16.3	—	—	—	—
Commercial (Wrought)**	60.0	42.0	—	10.0	35.0	—
SC51A						
Composite	22.7	17.6	26.3	1.7	0.8	0.8
Laboratory Casting*	23.5	—	31.9	—	—	—
Commercial (Casting)**	26.0	—	34.0	1.5	—	2.5

*The laboratory control castings contain 75% of the matrix alloy and
 25% 1100 Aluminum, which is the ratio of the matrix alloy and the
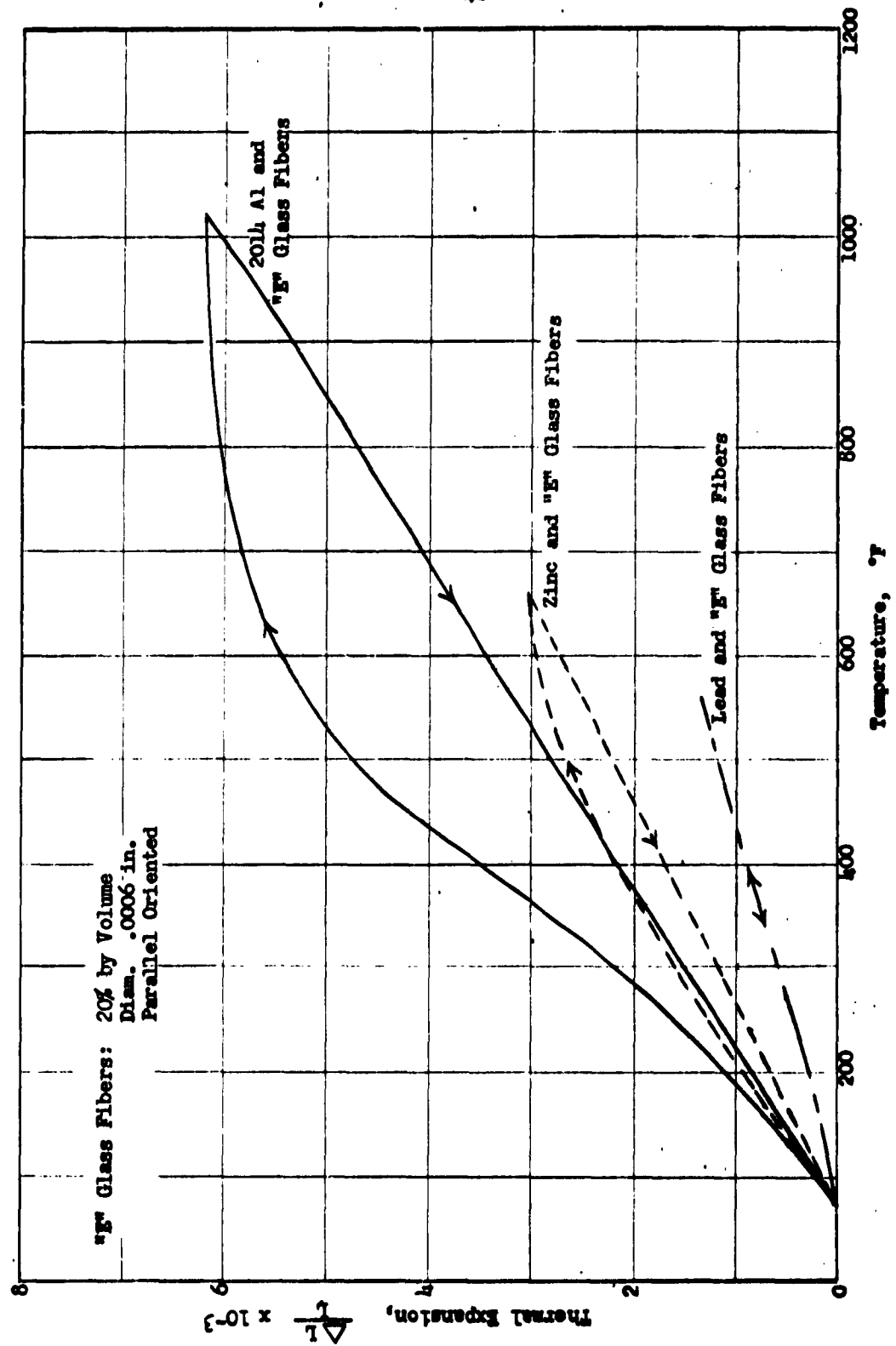 fiber coating alloy in composites.

**Handbook data.

Figure 10 – Thermal Expansion of Composites

A P P E N D I X B

TREATISE BY DR. E. SAIBEL

A Derivation of the Stress-Strain
Relationship of Composite Bars

A DERIVATION OF THE STRESS-STRAIN

RELATIONSHIP OF COMPOSITE BARS.

by

Edward Saibel

I. G. Tadjbakhsh

SUMMARY

A method has been developed by means of which stress-strain relation-ship of glass reinforced composite materials may be predicted from the stress-strain curves of the individual materials. The method is based on the fundamentals of the theory of elasticity and takes into account the non-linear behavior of materials. Flow curves have been determined for ordinary room temperature and at elevated temperatures.

Nomenclature

With the exception of symbols defined in the body of the paper the following nomenclature is used.

σ = uniaxial stress

σ_o = a universal constant taken as 4300 psi (see reference 1)

ε = uniaxial strain

σ_u = ultimate strength of metal

β = a constant dependent upon σ_u and σ_o (equation 3)

E_o = initial modulus of elasticity of metal i.e. at zero strain

E_m = instantaneous modulus of metal

E_g = modulus of elasticity of glass

T = temperature in degree Farenheit

ν = Poisson's ratio

Introduction

The fundamental problem is the behavior of a single glass fiber surrounded by a thin layer of metal coating under the application of an axial load. A composite bar with a high concentration of such glass fibers embedded in it, may then be assumed to act principally in the same manner that a single fiber does. In the following, first the separate behavior of the component parts will be examined and then the combined problem will be investigated.

Behavior of Metal

The coating metal being ordinarilly of aluminum compounds essentially exhibits a nonlinear stress-strain relationship when subjected to loads. This nonlinear behavior plays an important part in describing the behavior of composite bars especially at lower ranges of temperature where the strength of metal becomes comparable with that of glass. W. will take for the stress-strain relationship of the metal the following relationship (reference 1) which has been derived from phenomenological considerations of polycrystalline metals.

$$\sigma = \sigma_o \, \log_e \frac{\lambda_1 + \lambda_2 \, e^{-k\epsilon}}{\lambda_3 + \lambda_4 \, e^{-k\epsilon}} \tag{1}$$

where σ is the stress, ϵ is strain and σ is a universal constant and

$$\lambda_1 = \sqrt{1+\beta^2} + (1+\beta)$$

$$\lambda_2 = \sqrt{1+\beta^2} - (1+\beta)$$

$$\lambda_3 = \sqrt{1+\beta^2} + (1-\beta) \tag{2}$$

$$\lambda_4 = \sqrt{1+\beta^2} - (1-\beta)$$

$$k = \frac{E_0}{\sigma_0} \frac{\sqrt{1+\beta^2}}{\beta}$$

β being a constant described below.

Equation (1) is an isothermal relationship. For any given temperature of application of stress the constant β is related to the ultimate true strength of the metal at that temperature and is to be found from the relationship

$$\frac{\lambda_1}{\lambda_3} = e^{\sigma_u/\sigma_0} \tag{3}$$

If in addition the initial modulus of elasticity of the metal E_0 is known, all the required constants in equation (1) can be determined. The instantaneous modulus $E_m(\varepsilon) = d\sigma/d\varepsilon$ is given by

$$E_m = \frac{4E_0(1+\beta^2) e^{k\varepsilon}}{(\lambda_1 e^{k\varepsilon} + \lambda_2)(\lambda_3 e^{k\varepsilon} + \lambda_4)} \tag{4}$$

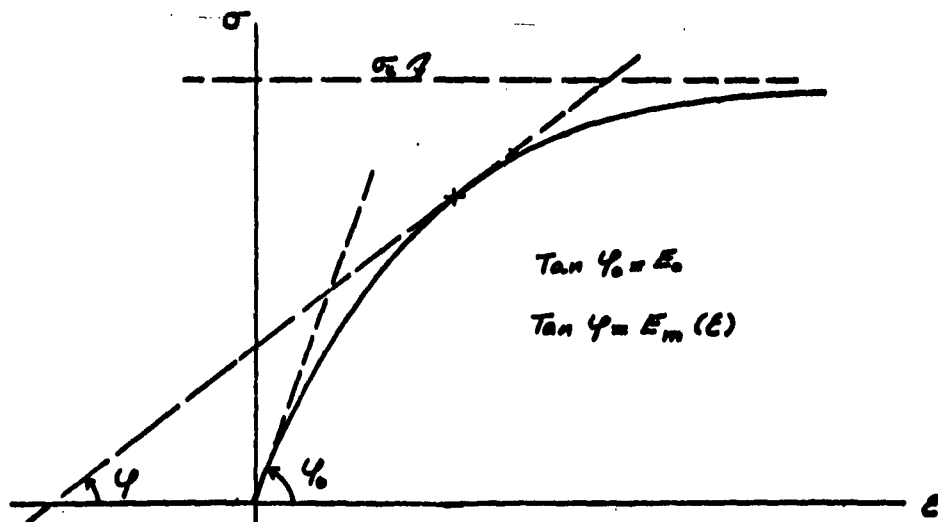Figure 1 illustrates all the characteristics of equation (1)

$Tan\ \varphi_o = E_o$

$Tan\ \varphi = E_m\ (\mathcal{E})$

Figure 1

For low temperatures ($75°F - 200°F$), σ_u is rather large and from

(3) $\quad \beta \gg 1 \quad$. In this case the preceeding equations can be some-

what simplified and take the following form

$$\sigma = \sigma_o\ log_e\ \frac{2\beta + 1}{1 + 2\beta\ exp\left(-\frac{E_o}{\sigma_o}\mathcal{E}\right)} \tag{5}$$

$$E_m = E_o\ \frac{2\beta}{2\beta + exp\left(\frac{E_o}{\sigma_o}\mathcal{E}\right)} \tag{6}$$

$$\beta = \frac{1}{2}\ exp\left(\frac{\sigma_u}{\sigma_o}\right) \tag{7}$$

However, when temperatures are rather high (200-700°F) β becomes comparable with unity and one must use the more accurate equations (3) and (4). For even higher temperatures these equations cease to be valid and creep must be taken into account.

Behavior of Glass

Glass is an almost perfect example of an elastic material. Its stress-strain relationship up to the point of breaking can be assumed to be

$$\sigma = E \varepsilon \tag{8}$$

or incrementally

$$d\sigma = E \, d\varepsilon \tag{9}$$

Furthermore its behavior changes very little with variation of temperature, for example its modulus of elasticity E_g changes by less than one percent in a rise of 250°F.

Stress-Strain Relationship for Composite Fiber

In many problems of mechanics a simple and straight forward approach often provides an adequate answer for the phenomenon under consideration along with the promise of being mathematically less cumbersome. A higher level of exactitude is warranted if experiment points to an inadequacy of the simpler approach. In the absence of sufficient experimental evidence, three different approaches have been adopted for this problem. In the first the effect of the difference of Poisson's ratio of the two media has been

neglected, in the second this effect has been taken into account while simplifying the problem by assuming that the metal coating is very thin. And in the third approach the complete problem has been considered. The final justification and limitation of any one of these approaches is of course dictated by experimental evidence.

A. Approach Number One

Consider the arrangement shown in Figure 2. The two media occupy the regions bounded by concentric circles of radii R_1 and R_2
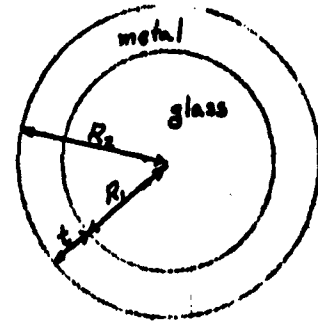
Figure 2

Let

A_m = area of metal

A_g = area of glass

P = load on fiber

σ_m = uniform stress in metal, equation (1) or (5)

σ_g = uniform stress in glass, equation (8)

$\mathcal{E}_m$ = axial strain in metal

$\mathcal{E}_g$ = axial strain in glass

Then assuming the condition of continuity in the form

$$\mathcal{E}_g = \mathcal{E}_m = \mathcal{E} \tag{10}$$

and neglecting the reduction of the areas due to Poisson ratio effect

we have

$$P = A_m \, \sigma_m + A_g \, \sigma_g \qquad (11)$$

or if we introduce

$$X_m = \frac{A_m}{A_m + A_g}$$

$$X_g = \frac{A_g}{A_m + A_g}$$

$$\sigma = \frac{P}{A_m + A_g} \qquad = \quad \text{observed stress}$$

we obtain with the aid of equations (1) and (8)

$$\sigma = X_m \left[\sigma_o \, \log_e \left| \frac{\lambda_1 + \lambda_2 \, e^{-k\varepsilon}}{\lambda_3 + \lambda_4 \, e^{-k\varepsilon}} \right| \right] + X_g \, E_g \, \varepsilon \qquad (12)$$

This equation should yield a good approximation in all cases in which the difference in Poisson's ratio of the materials is not too great. Its range of applicability should include single fibers and also composite bars which have a uniform distribution of glass fibers throughout their cross-sections.
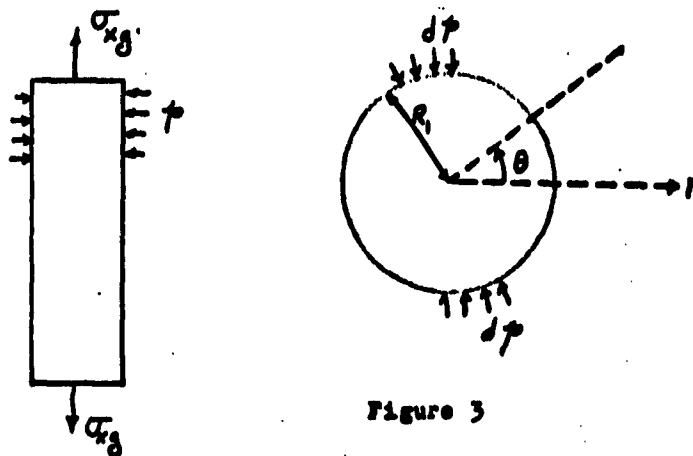
B. Approach Number Two

Figure 3

Assuming that at a certain instant of loading, a hydrostatic pressure p acts on the glass core, any further increase in load P will bring about a change in this pressure p. Then for the glass core we can write an incremental form of generalized Hooke's Law

$$d\varepsilon_{x_g} = \frac{1}{E_g}\left[d\sigma_{x_g} - \nu_g\left(d\sigma_{r_g} + d\sigma_{\theta_g}\right)\right] \tag{13}$$

$$d\varepsilon_{r_g} = \frac{1}{E_g}\left[d\sigma_{r_g} - \nu_g\left(d\sigma_{x_g} + d\sigma_{\theta_g}\right)\right] \tag{14}$$

but

$$d\sigma_{\theta_g} = d\sigma_{r_g} = -dp$$

Therefore

$$d\mathcal{E}_{x_g} = \frac{1}{E_g} \left[d\sigma_{x_g} + 2\nu_g \, dp \right] \tag{15}$$

$$d\mathcal{E}_{r_g} = -\frac{1}{E_g} \left[(1-\nu_g) \, dp + \nu_g \, d\sigma_{x_g} \right] \tag{16}$$

And for the metal when

$$R_1 \gg t$$

we can write in a similar manner (Fig. 4)
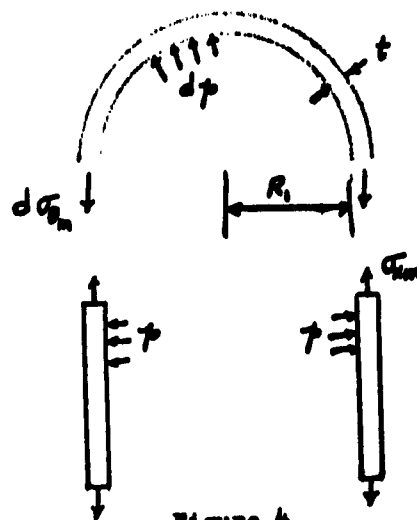
Figure 4

$$d\mathcal{E}_{x_m} = \frac{1}{E_m} \left[d\sigma_{x_m} - \nu_m (d\sigma_{\theta_m} + d\sigma_{r_m}) \right] \tag{17}$$

$$d\mathcal{E}_{r_m} = \frac{1}{E_m} \left[d\sigma_{r_m} - \nu_m (d\sigma_{x_m} + d\sigma_{\theta_m}) \right] \tag{18}$$

but approximately

$$d\sigma_{\theta_m} = \frac{R_1}{t} \, dp$$

$$d\sigma_{r_m} = -\frac{1}{2} \, dp$$

Therefore

$$d\,\mathcal{E}_{x_m} = \frac{1}{E_m}\left[d\,\sigma_{x_m} - \nu_m\left(\frac{R_1}{t} - \frac{1}{2}\right)d\rho\right] \qquad (19)$$

$$d\,\mathcal{E}_{r_m} = -\frac{1}{E_m}\left[\left(\frac{1}{2} + \nu_m\frac{R_1}{t}\right)d\rho + \nu_m\,d\sigma_{x_m}\right] \qquad (20)$$

Assuming that no slip and no separation occurs at the interface of the two media, we have as the requirements of continuity

$$d\,\mathcal{E}_{r_m} = d\,\mathcal{E}_{r_g} \qquad (21)$$

$$d\,\mathcal{E}_{x_m} = d\,\mathcal{E}_{x_g} = d\mathcal{E} \qquad (22)$$

The first of these implies

$$\frac{1}{E_g}\left[(1-\nu_g)d\rho + \nu_g\,d\sigma_{x_g}\right] = \frac{1}{E_m}\left[\left(\frac{1}{2} + \nu_m\frac{R_1}{t}\right)d\rho + \nu_m\,d\sigma_{x_m}\right]$$

from which

$$d\rho = \frac{1}{K}\left(\nu_g\,E_m\,d\sigma_{x_g} - \nu_m\,E_g\,d\sigma_{x_m}\right) \qquad (23)$$

where

$$K = E_g\left(\frac{1}{2} + \nu_m\frac{R_1}{t}\right) - E_m\left(1 - \nu_g\right) \qquad (24)$$

Substituting for dp in (16) and (20) we have

$$E_g \, d\ell = d\sigma_{x_g} + \frac{2\nu_g^2}{K} \left(\nu_g E_m \, d\sigma_{x_g} - \nu_m E_g \, d\sigma_{x_m} \right) \tag{25}$$

$$E_m \, d\ell = d\sigma_{x_m} - \frac{1}{K} \left(\frac{R_1}{t} - \frac{1}{2} \right) \left(\nu_g E_m \, d\sigma_{x_g} - \nu_m E_g \, d\sigma_{x_m} \right) \tag{26}$$

where use has been made of (22). Inverting these we get

$$d\sigma_{x_g} = \left(A E_m + E_g \right) d\ell \tag{27}$$

$$d\sigma_{x_m} = \left(-B E_m^2 + C E_m \right) d\ell \tag{28}$$

where

$$A = \frac{2\nu_g^2}{\nu_m} \div \left(\frac{R_1}{t} - \frac{1}{2} \right)$$

$$B = \frac{\left(1 - \nu_g - 2\nu_g^2 \right)}{\nu_m^2 E_g} \div \left(\frac{R_1}{t} - \frac{1}{2} \right) \tag{29}$$

$$C = \frac{\nu_g}{\nu_m} + \frac{1}{\nu_m^2} \left(\frac{1}{2} + \nu_m \frac{R_1}{t} \right) \div \left(\frac{R_1}{t} - \frac{1}{2} \right)$$

Let now

$dP =$ increment of applied load

$d\sigma = \dfrac{dP}{A_m + A_g} =$ increment in observed stress

Then equilibrium requires that

$$d\sigma = X_m \, d.\sigma_{xm} + X_g \, d\sigma_{xg} \tag{30}$$

or with the aid of (27) and (28)

$$d\sigma = \left[-BX_m E_m^2 + (C X_m + A X_g) E_m + X_g E_g \right] d\ell \tag{31}$$

where

$$E_m = 4E_0 (1+\beta^2) e^{k\ell} \div (\lambda_1 e^{k\ell} + \lambda_2)(\lambda_3 e^{k\ell} + \lambda_4)$$

For stress we have

$$\sigma = \int_0^\ell d\sigma$$

After carrying out the integration we obtain

$$\sigma = -X_m B E_0 \sigma_0 \left\{ \frac{\sqrt{1+\beta^2}}{\beta} \left(\frac{2c\,e^{-k\ell} + b}{a\,e^{k\ell} + c\,e^{-k\ell} + b} - T \right) + \right.$$

$$\left. \log_e \left| \frac{\lambda_2 e^{-k\ell} + \lambda_1}{\lambda_4 e^{-k\ell} + \lambda_3} \right| \right\} + (C X_m + A X_g) \log_e \left| \frac{\lambda_1 + \lambda_2 e^{-k\ell}}{\lambda_3 + \lambda_4 e^{-k\ell}} \right|$$

$$+ X_g E_g \ell \tag{32}$$

where

$$a = 2(1 + \sqrt{1+\beta^2}) , \quad b = 4\beta^2 , \quad c = 2(1 - \sqrt{1+\beta^2}) \tag{33}$$

$$T = (1 - \sqrt{1+\beta^2} + \beta^2) \div (1+\beta^2)$$

Thus within the framework of assumptions made, equation (32) represents the flow curve of a single glass fiber. As it stands this equation is not applicable for reinforced composite bars. For such bars, especially when the glass content is very low, metal coating around each single glass core is very thick and assumptions made regarding hoop and radial stresses no longer hold. For very high glass content one can consider the entire bar as a single fiber. In that case an equivalent (R_i/t) may be computed from

$$\left(\frac{t}{R_i}\right)^2 + 2\left(\frac{t}{R_i}\right) - \frac{X_m}{X_g} = 0$$

or   (34)

$$\frac{t}{R_i} = \sqrt{1 + \frac{X_m}{X_g}} - 1$$

C. Approach Number Three

N. I. Muskhelishvili (Reference 2) in his Mathematical Theory of Elasticity considers the problem of extension of a composite bar possessing rotational symmetry. If both bodies have linear stress-strain relationship, he gives the following formula for the magnitude of applied load, referring to figure (2)

$$P = (S_\varepsilon + K_{33})\varepsilon$$ (35)

where

$$S_\varepsilon = \pi R_i^2 E_1 + \pi(R_2^2 - R_i^2)E_2$$ (36)

$$K_{33} = \frac{4\pi(\nu_1 - \nu_2)^2(R_2^2 - R_i^2)R_i^2}{\gamma_1(R_2^4 - R_i^4) + \gamma_2 R_i^4 + 2\mu_2 R_2^2}$$ (37)

$$\gamma = \frac{2(1 - \nu - 2\nu^2)}{E} \quad , \quad \mu = \frac{1 + \nu}{E}$$

It is significant to notice that K_{33} is always a positive constant which adds to the rigidity of extension of the bar irrespective of the sign of ($\nu_1 - \nu_2^2$). In our notation equation (35) reads

$$\sigma = \left[\frac{D}{F + \frac{G}{E_m}} + X_m E_m + X_g E_g \right] \varepsilon \tag{38}$$

where

$$D = 4 \left(\nu_m - \nu_g \right)^2 X_g$$

$$F = \frac{2}{E_g} \left(1 - \nu_g - 2 \nu_g^2 \right) \tag{39}$$

$$G = 2 \left[\left(1 - \nu_m - 2 \nu_m^2 \right) \frac{X_g}{X_m} + \left(1 + \nu_m \right) \frac{1}{X_m} \right]$$

Writing equation (38) in the incremental form

$$d\sigma = \left[\frac{D}{F + \frac{G}{E_m}} + X_m E_m + X_g E_g \right] d\varepsilon \tag{40}$$

and integrating it in order to take into account the variation of E_m with strain we get after considerable mathematical manipulation

$$\sigma = \frac{H}{\gamma - \delta} \log_e \left| \frac{(e^{k\varepsilon} - \gamma)(1 - \delta)}{(e^{k\varepsilon} - \delta)(1 - \gamma)} \right| + X_m \sigma_0 \log_e \left| \frac{\lambda_1 + \lambda_2 e^{-k\varepsilon}}{\lambda_3 + \lambda_4 e^{-k\varepsilon}} \right|$$

$$+ X_g E_g \varepsilon \tag{41}$$

where

$$H = \frac{D}{2k\,\overset{*}{G}\,(1+\sqrt{1+\beta^2})} \qquad \overset{*}{G} = \frac{G}{4E_0\,(1+\beta^2)}$$

$$(p \cdot q) = \frac{1}{4(1+\sqrt{1+\beta^2})\,\overset{*}{G}}\left[-(F+4\beta^2\overset{*}{G}) \pm \sqrt{(F+4\beta^2\overset{*}{G})^2+16\beta^2\overset{*}{G}^2}\right]$$

The first term of equation (41) represents a correction to equation (12).

Conclusion

On the basis of theoretical analysis and numerical calculations a
few observations can be made regarding the stress-strain relationships
derived above. Equation (12) provides a relatively simple means of pre-
dicting flow curves for single fibers as well as for composite bars, and
in all cases where the difference in Poisson's ratio of the two materials
may be neglected. The use of equation (32) is to be confined to single
fibers and composite bars of more than 70% glass of uniform distribution.
Equation (41) is more cumbersome to evaluate numerically but is applica-
ble to single fibers as well as to composite bars of uniform glass
distribution. In the case of bars with 20% glass it has been found that
equations (12) and (41) almost coincide. The difference is very small.

It must be pointed out that the three methods of approach explained
above are really various degrees of approximation to the actual problem,
starting with elementary considerations and ending with more accurate
methods in which the interaction of the two media has been considered.

Examples

For purposes of illustration and comparison the following numerical examples have been worked out for equations (12), (32) and (41).

General Data

T = temperature = $500°F$

σ_u = ultimate strength of 2a-H12 aluminum = 4300 psi

E_0 = initial modulus of metal = 7.8×10^6 psi

ν_m = 0.33

E_g = modulus of glass = 11.3×10^6 psi

ν_g = 0.2

σ_b = a universal constant = 4300 psi (see reference 1)

Then from (2) and (3)

β = 1.1752

λ_1 = 3.718

λ_2 = -0.632

λ_3 = 1.368

λ_4 = 1.718

k = 2.382×10^3

and from (33)

a = 5.086

b = 5.524

c = 1.086

T = 0.349

I. <u>Single glass fiber (30% metal, 70% glass)</u>

$$R_1 = 2.5 \times 10^{-4} \text{ inches}$$

$$t = 0.5 \times 10^{-4} \text{ inches}$$

$$X_g = 0.7$$

$$X_m = 0.3$$

from (29)

$$A = 0.269$$

$$B = 0.141 \times 10^{-6}$$

$$C = 5.4$$

$$C X_m + A X_g = 1.81$$

II. <u>Composite bar (80% metal, 20% glass)</u>

$$X_m = 0.8$$

$$X_g = 0.2$$

$$t/R_1 = -1 + \sqrt{1 + \frac{X_m}{X_g}} = 1.236$$

$$R_1/t = 0.809$$

$$A = 3.883$$

$$B = 2.063 \times 10^{-6} \quad \text{in}^2/\text{lb}.$$

$$C = 25.492$$

$$C X_m + A X_g = 21.17$$

and

$$D = 0.01352$$

$$F = 1.274 \times 10^{-7} \quad \text{in}^2/\text{lb}$$

$$G = 2.56$$

$$G^{*} = 0.3446 \times 10^{-7} \quad \text{in.}^2 / lb.$$

$$\frac{D}{8k\,G^n \left(1 + \sqrt{4\gamma\beta^2}\right)} = 0.0324 \times 10^{3} \text{ psi}$$

$$\gamma = 0.111$$

$$\beta = -1.922$$

Numerical Data for Stress-Strain Curves

T=500°?, 2S-H12 Aluminum, "E" Glass

ε Strain	σ_g psi Eq.(8)	σ_m psi Eq.(1)	σ 30% metal psi Eq.(12)	Eq.(32)	σ Eq.(12)	σ 8 Eq.
0.2×10^{-3}	2.26×10^3	1.34×10^3	1.98×10^3	3.65×10^3	1.52×10^3	24
0.4	4.52	2.309	3.857	6.75×10^3	2.751	
0.6	6.78	2.988	5.642	9.454	3.746	5
0.8	9.04	3.453	7.364	11.842	4.57	6
1.0	11.3	3.762	9.038	13.962	5.27	7
1.4	15.82	4.085	12.3	17.701	6.432	7
1.8	20.34	4.214	15.502	21.098	7.439	8
2.0	22.6	4.244	17.1	22.735	7.92	8
2.5	28.25	4.287	21.06	26.764	9.03	8
3.0	33.9	4.296	25.02	30.736	10.22	8
3.5	39.55	4.3	28.98	34.698	11.35	8
4.0	45.2	4.3	32.93	38.653	12.48	8
5	56.5	4.3				
6	67.8	4.3	48.75	54.473	17.0	9
7	79.1	4.3				
10	113	4.3				
15	169.5	4.3	119.94	125.663	37.34	1
20	226	4.3		165.21		
25	282.5	4.3			59.94	1
30	339	4.3	238.29	244.0	7...	
40	452	4.3				

References

1. Stowell, E. Z. A Phenomenological Relation between Stress, Strain

    rate, and temperature for Metals at Elevated Temperatures N.A.C.A.

    Technical Note No. 4000, 1957.

2. Muskhelishvili, N. I. Some Basic Problems of Mathematical Theory

    of Elasticity. P. Noordhoff Ltd., Goringen, Holland, P. 647. 1953.